



IN-02  
390162

# TECHNICAL NOTE

D-1145

ATMOSPHERE ENTRIES WITH VEHICLE LIFT-DRAG RATIO  
MODULATED TO LIMIT DECELERATION AND RATE OF  
DECELERATION - VEHICLES WITH MAXIMUM  
LIFT-DRAG RATIO OF 0.5

By Elliott D. Katzen and Lionel L. Levy, Jr.

Ames Research Center  
Moffett Field, Calif.

NATIONAL AERONAUTICS AND SPACE ADMINISTRATION  
WASHINGTON

December 1961

## NATIONAL AERONAUTICS AND SPACE ADMINISTRATION

## TECHNICAL NOTE D-1145

## ATMOSPHERE ENTRIES WITH VEHICLE LIFT-DRAG RATIO

## MODULATED TO LIMIT DECELERATION AND RATE OF

## DECELERATION - VEHICLES WITH MAXIMUM

## LIFT-DRAG RATIO OF 0.5

By Elliott D. Katzen and Lionel L. Levy, Jr.

## SUMMARY

An analysis has been made of atmosphere entries for which the vehicle lift-drag ratio was modulated to maintain specified maximum decelerations and/or maximum deceleration rates. The part of the vehicle drag polar used during modulation was from maximum lift coefficient to minimum drag coefficient. The entries were at parabolic velocity and the vehicle maximum lift-drag ratio was 0.5. Two-dimensional trajectory calculations were made for a nonrotating, spherical earth with an exponential atmosphere. The results of the analysis indicate that for a given initial flight-path angle, modulation generally resulted in a reduction of the maximum deceleration to 60 percent of the unmodulated value or a reduction of maximum deceleration rate to less than 50 percent of the unmodulated rate. These results were equivalent, for a maximum deceleration of  $10g$ , to lowering the undershoot boundary 24 miles with a resulting decrease in total convective heating to the stagnation point of 22 percent. However, the maximum convective heating rate was increased 18 percent; the maximum radiative heating rate and total radiative heating were each increased about 10 percent.

## INTRODUCTION

Man's performance of useful duties during atmosphere entry requires that the decelerations and the deceleration rates be kept within prescribed limits. For nonlifting vehicles, the limiting of deceleration and deceleration rates by modulation of drag has been treated in references 1, 2, and 3. For lifting vehicles, limited studies of the effects of modulation of lift and drag to limit the deceleration were made in references 4 and 5. More extensive studies were made in references 6 and 7 but, admittedly, the reductions in maximum deceleration afforded by the use of modulation were conservative, especially for vehicles with maximum lift-drag ratio as low as 0.5, because of the assumptions on which the analyses were based. Information on the limiting of deceleration rates by modulation, for lifting vehicles, has not been available.

The purpose of the present report is to answer the following questions: Given a manned vehicle with a maximum lift-drag ratio of 0.5 entering the earth's atmosphere at a given flight-path angle, how much can the deceleration and rate of deceleration be reduced by modulation, and what are the corresponding changes in convective and radiative heating and range? To answer these questions a trajectory analysis has been made on an IBM 704 computing machine to solve the two-dimensional equations of motion of reference 8. The results obtained are for parabolic entry velocity, a nonrotating spherical earth, and an exponential atmosphere. The results are applicable to vehicles that can be operated in the angle-of-attack range from maximum lift coefficient to minimum drag coefficient.

#### NOTATION

A	reference area for drag and lift, ft <sup>2</sup>
C <sub>D</sub>	drag coefficient, $\frac{2D}{\rho V^2 A}$
C <sub>D0</sub>	drag coefficient at zero lift
C <sub>L</sub>	lift coefficient, $\frac{2L}{\rho V^2 A}$
D	drag force, lb
g	local gravitational acceleration, ft sec <sup>-2</sup>
G	deceleration in g units
L	lift force, lb
m	mass of vehicle, slugs
q	total heat absorbed at the stagnation point, Btu ft <sup>-2</sup>
$\dot{q}$	heating rate at the stagnation point, $\frac{dq}{dt}$ , Btu ft <sup>-2</sup> sec <sup>-1</sup>
r	distance from the center of planet, ft
r <sub>0</sub>	radius of planet, 2.0926×10 <sup>7</sup> ft for earth
R	radius of curvature of vehicle surface, ft
s	range, ft
t	time, sec

$u$	tangential velocity component normal to a radius vector, $\text{ft sec}^{-1}$
$v$	radial velocity component, $\text{ft sec}^{-1}$
$V$	resultant velocity, $\text{ft sec}^{-1}$
$y$	altitude, $\text{ft}$
$\alpha$	angle of attack of vehicle, $\text{deg}$
$\beta$	atmosphere density decay parameter, $1/23,500 \text{ ft}^{-1}$ for earth
$\gamma$	flight-path angle relative to the local horizontal, negative for descent, $\text{deg}$
$\mu$	gravitational constant, $1.4078 \times 10^{16} \text{ ft}^3 \text{sec}^{-2}$ for earth
$\rho$	atmosphere density, $\text{slugs ft}^{-3}$
$\rho_0$	atmosphere density at planet surface, $0.00238 \text{ slug ft}^{-3}$ for earth
$\bar{\rho}_0$	mean value for exponential approximation to atmosphere density-altitude relation, $0.0027 \text{ slug ft}^{-3}$ for earth

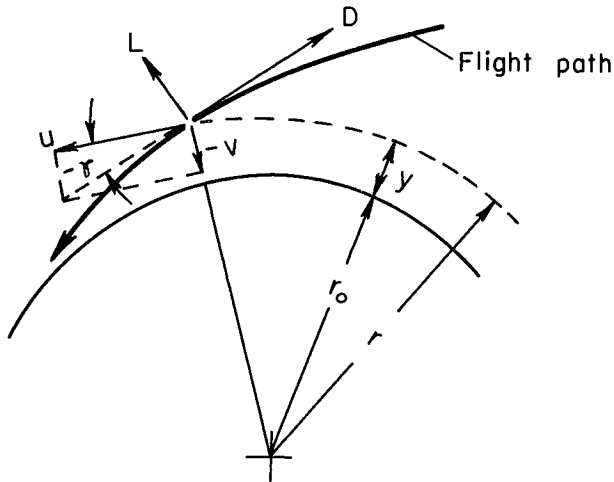
#### Subscripts

$c$	convective
$i$	initial
$\text{max}$	maximum
$p$	vacuum perigee
$r$	radiative

#### ANALYSIS

##### Trajectory Equations

A trajectory analysis has been made utilizing the solution of two-dimensional equations of motion for entries into an exponential atmosphere of a nonrotating spherical earth. The polar coordinate system with velocity components, aerodynamic forces, and flight-path angle is defined



in the sketch. The differential equations for the velocity in the radial and tangential directions are, respectively, (see ref. 8)

$$\frac{dv}{dt} = -g + \frac{u^2}{r} + \frac{L}{m} \cos \gamma - \frac{D}{m} \sin \gamma \quad (1)$$

$$\frac{du}{dt} = -\frac{uv}{r} - \frac{D}{m} \cos \gamma - \frac{L}{m} \sin \gamma \quad (2)$$

where

$$\tan \gamma = \frac{v}{u} \quad (3)$$

$$r = r_0 + y \quad (4)$$

and  $g$  is the local gravitational acceleration given by

$$g = \frac{\mu}{r^2} \quad (5)$$

The constant  $\mu$  in equation (5) is the gravitational constant defined by Newton's inverse square law of gravitational attraction. The differential equations employed for the altitude and range are, respectively,

$$\frac{dy}{dt} = v \quad (6)$$

$$\frac{ds}{dt} = u \quad (7)$$

The differential equations used for the total laminar convective heat (after ref. 8) and the radiative heat (ref. 9) absorbed per unit area at the stagnation point are, respectively,

$$\frac{dq_c}{dt} = \dot{q}_c = \frac{16,600}{\sqrt{R}} \sqrt{\frac{\rho}{\rho_0}} \left( \frac{V}{\sqrt{gr}} \right)^3 \quad (8)$$

$$\frac{dq_r}{dt} = \dot{q}_r = R10^f(y, V) \quad (9)$$

where  $R$  is the radius of curvature of the vehicle surface at the stagnation point,  $\rho$  is the local atmosphere density given by

$$\rho = \bar{\rho}_0 e^{-\beta y} \quad (10)$$

$u$	tangential velocity component normal to a radius vector, $\text{ft sec}^{-1}$
$v$	radial velocity component, $\text{ft sec}^{-1}$
$V$	resultant velocity, $\text{ft sec}^{-1}$
$y$	altitude, $\text{ft}$
$\alpha$	angle of attack of vehicle, $\text{deg}$
$\beta$	atmosphere density decay parameter, $1/23,500 \text{ ft}^{-1}$ for earth
$\gamma$	flight-path angle relative to the local horizontal, negative for descent, $\text{deg}$
$\mu$	gravitational constant, $1.4078 \times 10^{16} \text{ ft}^3 \text{sec}^{-2}$ for earth
$\rho$	atmosphere density, $\text{slugs ft}^{-3}$
$\rho_0$	atmosphere density at planet surface, $0.00238 \text{ slug ft}^{-3}$ for earth
$\bar{\rho}_0$	mean value for exponential approximation to atmosphere density-altitude relation, $0.0027 \text{ slug ft}^{-3}$ for earth

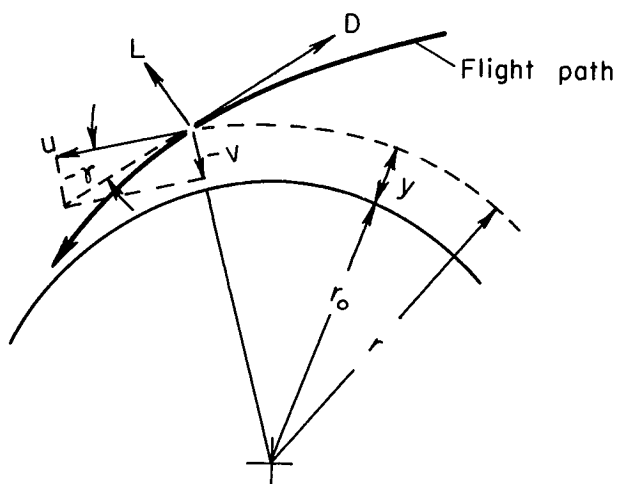
#### Subscripts

$c$	convective
$i$	initial
$\text{max}$	maximum
$p$	vacuum perigee
$r$	radiative

#### ANALYSIS

##### Trajectory Equations

A trajectory analysis has been made utilizing the solution of two-dimensional equations of motion for entries into an exponential atmosphere of a nonrotating spherical earth. The polar coordinate system with velocity components, aerodynamic forces, and flight-path angle is defined



in the sketch. The differential equations for the velocity in the radial and tangential directions are, respectively, (see ref. 8)

$$\frac{dv}{dt} = -g + \frac{u^2}{r} + \frac{L}{m} \cos \gamma - \frac{D}{m} \sin \gamma \quad (1)$$

$$\frac{du}{dt} = -\frac{uv}{r} - \frac{D}{m} \cos \gamma - \frac{L}{m} \sin \gamma \quad (2)$$

where

$$\tan \gamma = \frac{v}{u} \quad (3)$$

$$r = r_0 + y \quad (4)$$

and  $g$  is the local gravitational acceleration given by

$$g = \frac{\mu}{r^2} \quad (5)$$

The constant  $\mu$  in equation (5) is the gravitational constant defined by Newton's inverse square law of gravitational attraction. The differential equations employed for the altitude and range are, respectively,

$$\frac{dy}{dt} = v \quad (6)$$

$$\frac{ds}{dt} = u \quad (7)$$

The differential equations used for the total laminar convective heat (after ref. 8) and the radiative heat (ref. 9) absorbed per unit area at the stagnation point are, respectively,

$$\frac{dq_c}{dt} = \dot{q}_c = \frac{16,600}{\sqrt{R}} \sqrt{\frac{\rho}{\rho_0}} \left( \frac{v}{\sqrt{gr}} \right)^3 \quad (8)$$

$$\frac{dq_r}{dt} = \dot{q}_r = R10^f(y, v) \quad (9)$$

where  $R$  is the radius of curvature of the vehicle surface at the stagnation point,  $\rho$  is the local atmosphere density given by

$$\rho = \bar{\rho}_0 e^{-\beta y} \quad (10)$$

and  $V$  is the resultant velocity given by

$$V = \sqrt{u^2 + v^2} \quad (11)$$

The radiative heating rate per unit area at the stagnation point is obtained from an interpolation of a table for the logarithm of equation (9), that is,

$$\log_{10} \left( \frac{\dot{q}_r}{R} \right) = f(y, V) \quad (12)$$

Values of  $(\dot{q}_r/R)$  as a function of altitude and velocity for air in equilibrium were obtained from reference 9.

The six equations (1), (2), (6), (7), (8), and (9) were programed for simultaneous solution on an IBM 704 computing machine for entries during which the vehicle aerodynamic coefficients were constant and for entries during which these coefficients were varied (modulated) in order to satisfy specified constraints of a maximum deceleration rate and/or a maximum deceleration. The modulation started at  $C_{L_{max}}$  and ended at  $C_{D_0}$  because this type of modulation provides the lowest possible maximum deceleration (see, e.g., ref. 6). In the analysis the resultant deceleration  $G$  is given by

$$G = \frac{\bar{p}_0}{2\mu(m/A)} r^2 e^{-\beta y} V^2 C_D \sqrt{1 + \left( \frac{L}{D} \right)^2} \quad (13)$$

For entries modulated to maintain a specified maximum deceleration rate, the deceleration time history during the modulation period is linear, that is,

$$\frac{dG}{dt} = \text{constant} \quad (14)$$

and for entries modulated to maintain a specified maximum deceleration, the deceleration is constant during the modulation period.

#### Vehicle Characteristics

Modulation is accomplished in the present investigation by varying the vehicle drag coefficient and lift-drag ratio during entry. The drag coefficient and lift-drag ratio are calculated on the assumption (as in ref. 4) that the vehicle has a variation of lift and drag similar to that for a flat plate in Newtonian flow given by



$$C_D = C_{D_0} + (C_{D_{\max}} - C_{D_0}) \sin^3 \alpha \quad (15)$$

$$C_L = (C_{D_{\max}} - C_{D_0}) \sin^2 \alpha \cos \alpha \quad (16)$$

$$\frac{L}{D} = \frac{\sin^2 \alpha \cos \alpha}{b + \sin^3 \alpha} \quad (17)$$

where

$$b = \frac{C_{D_0}}{C_{D_{\max}} - C_{D_0}}$$

The particular drag polar with a maximum lift-drag ratio of 0.5 used in the present investigation is given in figure 1. The results, however, can be shown to apply to a family of vehicles having  $(L/D)_{\max} = 0.5$  with various values of  $C_{D_{\max}}$  and  $C_{D_0}$  provided  $C_{D_{\max}}/C_{D_0}$  remains constant and the initial  $m/A$  is adjusted to give initial values of  $m/C_D A$  equal to those used in the present investigation. A value of  $m/A = 3$  was used in the present calculations.

The results of the present analysis can be applied to vehicles of arbitrary weight and size by employing the results of reference 8. According to these results, many of the trajectory parameters are essentially independent of  $m/C_D A$ . In this category are deceleration, deceleration rate, velocity, flight-path angle, and range. Trajectory parameters that depend on  $m/C_D A$  are altitude and convective and radiative heating where the relationships for altitude and convective heating can be shown to be

$$y_2 - y_1 = \frac{1}{\beta} \log_e \left[ \frac{(m/C_D A)_1}{(m/C_D A)_2} \right] \quad (18)$$

and

$$\frac{q_{c2}}{q_{c1}} \sim \frac{\dot{q}_{c2}}{\dot{q}_{c1}} \sim \sqrt{\frac{(m/C_D AR)_2}{(m/C_D AR)_1}} \quad (19)$$

The subscript 1 refers to values of the present report and the subscript 2 corresponds to other values of  $m/C_D A$  or  $m/C_D AR$ . Equations (9) and (18) and reference 9 can be used to calculate radiative heating if the velocity-time and velocity-altitude relationships are given.

## Corridor Depth

In general, corridor depth is defined as a difference in perigee altitudes of vacuum trajectories corresponding to a difference in two flight-path angles at a given initial altitude and velocity. The flight-path angle associated with the higher of the two perigee altitudes is usually referred to as the angle for an overshoot boundary, and the angle associated with the lower of the two perigee altitudes is referred to as the angle for an undershoot boundary (see, e.g., ref. 4). The relationship between perigee altitude and flight-path angle for a vehicle at parabolic velocity can be shown from vacuum trajectory relationships to be

$$y_p = y_i \cos^2 \gamma_i - r_o(1 - \cos^2 \gamma_i) \quad (20)$$

Perigee altitude and corridor depth are presented as functions of flight-path angle in figure 2 for an initial altitude of 400,000 feet. A corridor depth of zero was chosen so that it corresponded to  $\gamma = -5.03^\circ$ . This is defined as the overshoot boundary in the present report since the vehicle entering at its highest negative lift-drag ratio (-0.5) skips out of the atmosphere for entries with angles of descent less than  $5.03^\circ$ .

## RESULTS AND DISCUSSION

In order to determine the effects of modulation of lift and drag for a vehicle entering the earth's atmosphere at parabolic velocity, unmodulated and modulated trajectories have been computed. Unmodulated entries are defined in this report as entries during which the lift-drag ratios are held constant until the flight path is essentially horizontal ( $\gamma \approx 0$ , near maximum deceleration). To prevent skipping out of the atmosphere for the unmodulated entries with  $L/D = 0.5$ , step changes to  $L/D = -0.5$  then back to  $L/D = 0.5$  were programed to occur at points along the flight path so that decelerations greater than the first peak decelerations were avoided. To prevent excessive decelerations for the unmodulated overshoot entry with  $L/D = -0.5$ , a step change to  $L/D = 0$ ,  $\alpha = 90^\circ$ , was made at  $\gamma \approx 0$ . For the modulated trajectories, the initial lift-drag ratio was 0.42, the value for maximum lift coefficient. Two types of modulation were employed; one held the maximum deceleration to a specified value, the other held the maximum deceleration rate to a specified value, with a further stipulation that a maximum deceleration of  $10g$  was not to be exceeded.

In figure 3 typical modulated trajectories are compared with an unmodulated trajectory having identical initial conditions. Results from these and similar trajectories have been compiled to provide a summary of the effect of modulation on maximum deceleration and deceleration rate, total and peak stagnation point heating, and range.

### Maximum Deceleration

Figure 4 shows the maximum decelerations for unmodulated and modulated entries as functions of corridor depth and initial flight-path angle. For the unmodulated entries the maximum decelerations increased with increased corridor depth and decreased with increased lift-drag ratio as has been found previously (e.g., refs. 4, 5, and 8). For fixed corridor depth, the use of modulation provided reductions of maximum deceleration to values that were approximately 60 percent of the lowest unmodulated values ( $L/D = 0.5$ ). A few trajectories were also computed for initial velocities from 15,000 to 50,000 feet per second and the same reduction in maximum deceleration was found. For entries at escape velocity with a maximum deceleration limit of  $10g$ , the above reduction in maximum deceleration is equivalent to lowering the undershoot boundary 24 miles. Thus, if the vehicle were operated at  $L/D = -0.5$  on the overshoot boundary and modulation were used to enter at the steepest possible angle and not exceed  $10g$ , the resulting corridor depth would be 62 statute miles.

It is of interest to note that if modulation is attempted to reduce the maximum deceleration to values below those of the lowest curve of figure 4, a maneuver might be required after reaching  $\alpha = 0^\circ$  to prevent maximum decelerations greater than that experienced if modulation had not been used. This is illustrated in figure 5 which shows the maximum deceleration obtained by modulation as a function of the maximum deceleration desired by modulation for an initial flight-path angle of  $-8.14^\circ$  (corresponding to a corridor depth of 50 miles). The maximum deceleration for an unmodulated entry under these conditions with  $L/D = 0.5$  was about  $13.2g$ . It can be seen from figure 5 that if modulation is attempted to hold the maximum deceleration to less than about  $7g$ , the maximum deceleration will exceed the maximum deceleration for the unmodulated entry. This occurs because the rate of decrease of angle of attack required is so great that the flight-path angle is still relatively steep when the vehicle is operating at  $0^\circ$  angle of attack. Decelerations higher than those for the unmodulated case can be avoided, however, by an increase in angle of attack after  $\alpha = 0^\circ$  is reached.

### Maximum Deceleration Rate

Figure 6 shows the maximum rates of increase of deceleration for unmodulated and modulated entries as functions of corridor depth and entry angle. For corridor depths up to about 44 miles, modulation was used to reduce the deceleration rates as much as possible without regard to the maximum decelerations. For corridor depths from 44 to 62 miles, modulation was used to reduce the deceleration rates as much as possible and still limit the maximum deceleration to  $10g$ . For a given corridor depth, the deceleration rates were generally reduced to less than half the values for the unmodulated entries with  $L/D = (L/D)_{\max} = 0.5$ . It can also be seen from figure 6 that an undershoot boundary that is limited by a maximum

deceleration of 10g and a maximum deceleration rate of 0.5g per second (38 mile corridor depth) can be lowered 20 miles (58 mile corridor depth) by modulation. This is only 4 miles (62 mile corridor depth) less than the undershoot boundary limited by a maximum deceleration rate of over 1g per second.

### Stagnation-Point Heating

Maximum convective heating rate.- The maximum laminar convective heating rates for the unmodulated and modulated entries are shown in figure 7 as functions of corridor depth and entry angle. The heating rates generally increased with increasing corridor depth and entry angle. For a given corridor depth, the heating rates were approximately the same for the unmodulated entries with  $L/D = 0.5$  and the entries modulated to limit the deceleration; modulation to limit the deceleration rate generally resulted in heating rates about 20 percent higher than those for the unmodulated  $L/D = 0.5$  entries. Modulation to lower the 10g-limited undershoot boundary 24 miles (corridor depth increase from 38 to 62 miles) resulted in an 18-percent increase in peak convective heating rate.

Maximum radiative heating rate.- The maximum radiative heating rates for the unmodulated and modulated entries are presented in figure 8 as functions of corridor depth and entry angle. The radiative heating rates generally increased with increasing corridor depth and entry angle. However, for a given corridor depth, the peak radiative heating rates for the unmodulated entries with  $L/D = 0.5$  were considerably higher than the rates for the entries modulated to limit the maximum deceleration. Modulation to lower the 10g-limited undershoot boundary 24 miles resulted in about a 10-percent increase in peak radiative heating rate.

Total convective heating.- The effect of modulation on the total convective heat absorbed per unit area at the stagnation point is shown in figure 9. To obtain the total heat for the unmodulated entries with  $L/D = 0.5$ , the vehicle was maneuvered as described earlier. Trajectories were also calculated for other maneuvers after peak deceleration to keep the vehicle from skipping out of the atmosphere; for these maneuvers the total heat was about the same or greater than that shown. It can be seen from figure 9 that modulation to lower the 10g undershoot boundary 24 miles resulted in a decrease in total convective heating of 22 percent.

Total radiative heating.- It can be seen from figure 10 that modulation to lower the 10g undershoot boundary 24 miles resulted in about a 10-percent increase in total radiative heating. Modulation to limit the deceleration rate for initial flight-path angles such that  $G_{\max} < 10$ , however, resulted in much larger increases in total radiative heating.

## Range

It is evident from figure 11 that the range increased very rapidly for the unmodulated and modulated entries as the corridor depth or flight-path angle was decreased to such values that the vehicle was about to skip out of the atmosphere. Modulation to lower the 10g undershoot boundary 24 miles resulted in a decrease in range of about 60 percent.

## CONCLUDING REMARKS

Unmodulated and modulated trajectories have been computed for a vehicle having a maximum lift-drag ratio of 0.5 entering the earth's atmosphere at parabolic velocity. The results indicate that modulation can reduce the maximum deceleration to 60 percent of the unmodulated value or reduce the maximum deceleration rate to less than 50 percent of the unmodulated rate. These results are equivalent, for a maximum deceleration of 10g, to lowering the undershoot boundary 24 miles with a resulting decrease in total convective heating to the stagnation point of 22 percent. However, the maximum convective heating rate was increased 18 percent; the maximum radiative heating rate and total radiative heating were each increased about 10 percent.

Ames Research Center  
National Aeronautics and Space Administration  
Moffett Field, Calif., Sept. 11, 1961

## REFERENCES

1. Levy, Lionel L., Jr.: An Approximate Analytical Method for Studying Atmosphere Entry of Vehicles With Modulated Aerodynamic Forces. NASA TN D-319, 1960.
2. Levy, Lionel L., Jr.: The Use of Drag Modulation to Limit the Rate at Which Deceleration Increases During Nonlifting Entry. NASA TN D-1037, 1961.
3. Phillips, Richard L., and Cohen, Clarence B.: Use of Drag Modulation to Reduce Deceleration Loads During Atmospheric Entry. Space Tech. Labs. Rep. GM-TR-0165-00352, April 1958.
4. Chapman, Dean R.: An Analysis of the Corridor and Guidance Requirements for Supercircular Entry Into Planetary Atmospheres. NASA TR R-55, 1960.

5. Lees, Lester, Hartwig, Frederick W., and Cohen, Clarence B.: The Use of Aerodynamic Lift During Entry Into the Earth's Atmosphere. Space Tech. Labs. Rep. GM-TR-0165-00519, Nov. 1958. (Also GALCIT Pub. 462, and Amer. Rocket Soc. Jour., vol. 29, no. 9, Sept. 1959, pp. 633-641.)
6. Grant, Frederick C.: Modulated Entry. NASA TN D-452, 1960.
7. Luidens, Roger W.: Approximate Analysis of Atmospheric Entry Corridors and Angles. NASA TN D-590, 1961.
8. Chapman, Dean R.: An Approximate Analytical Method for Studying Entry Into Planetary Atmospheres. NASA TR R-11, 1959.
9. Yoshikawa, Kenneth K., and Wick, Bradford H.: Radiative Heat Transfer During Atmosphere Entry at Parabolic Velocity. NASA TN D-1074, 1961.

A  
5  
6  
4

4  
3  
2  
1

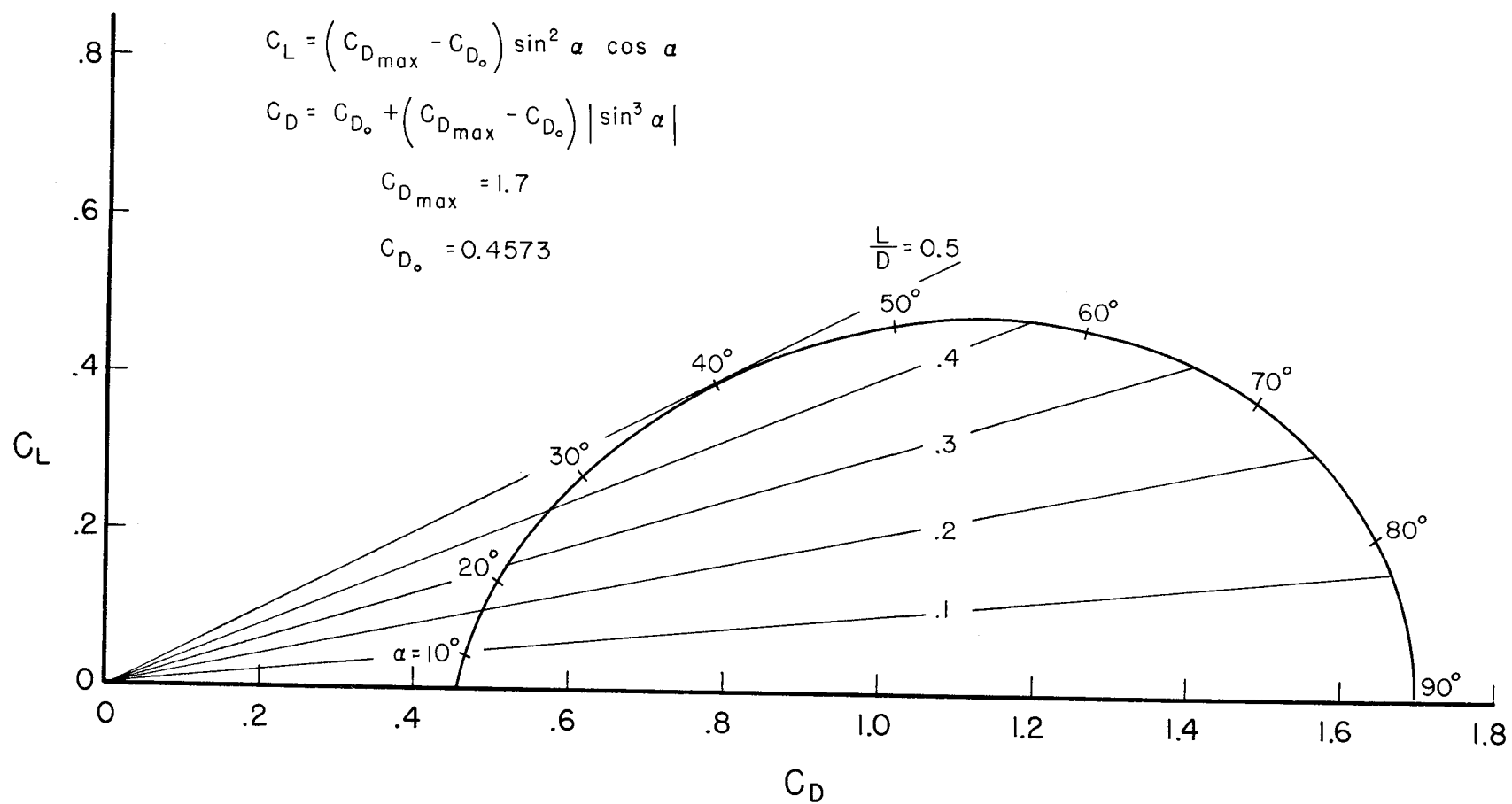


Figure 1.- Drag polar.



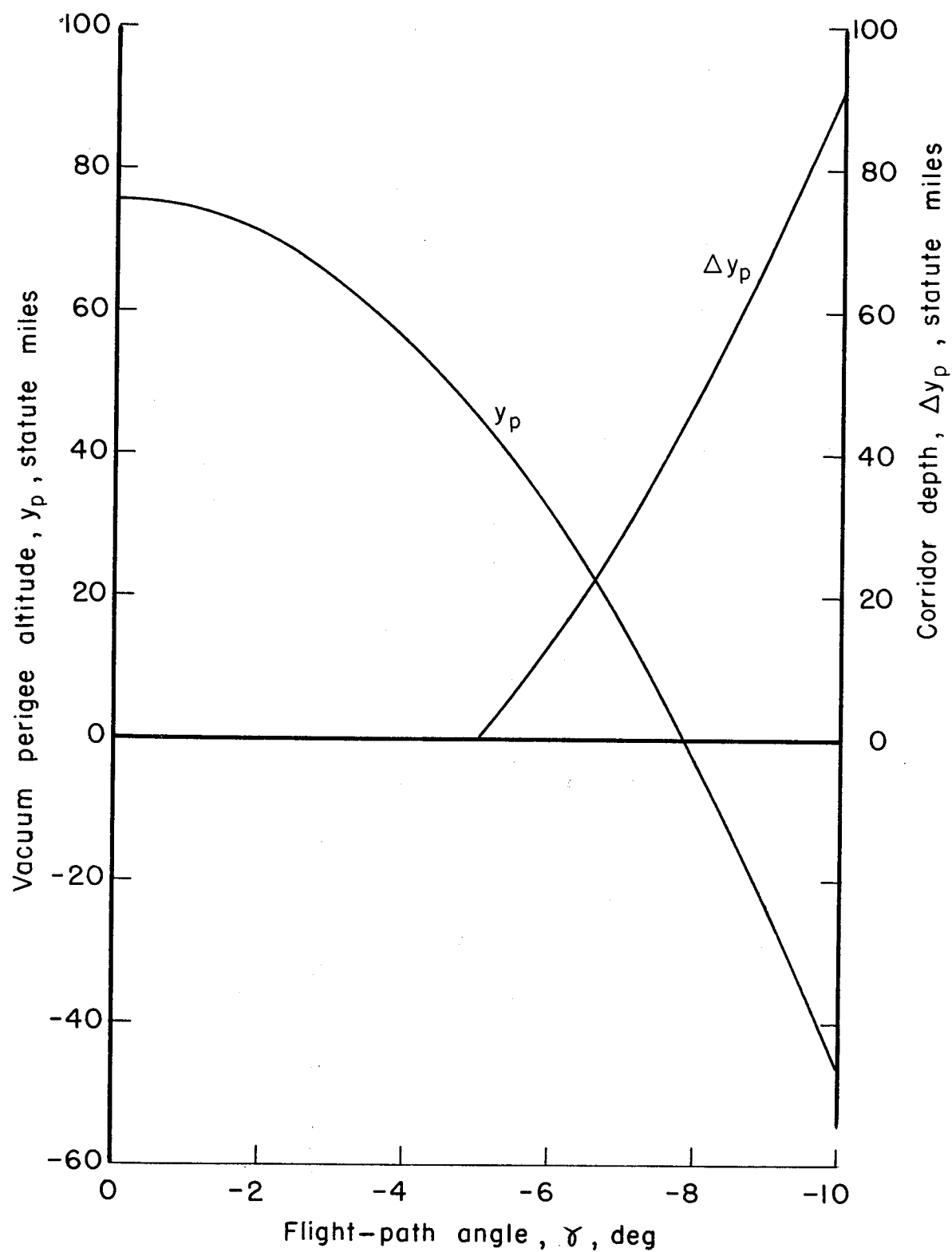
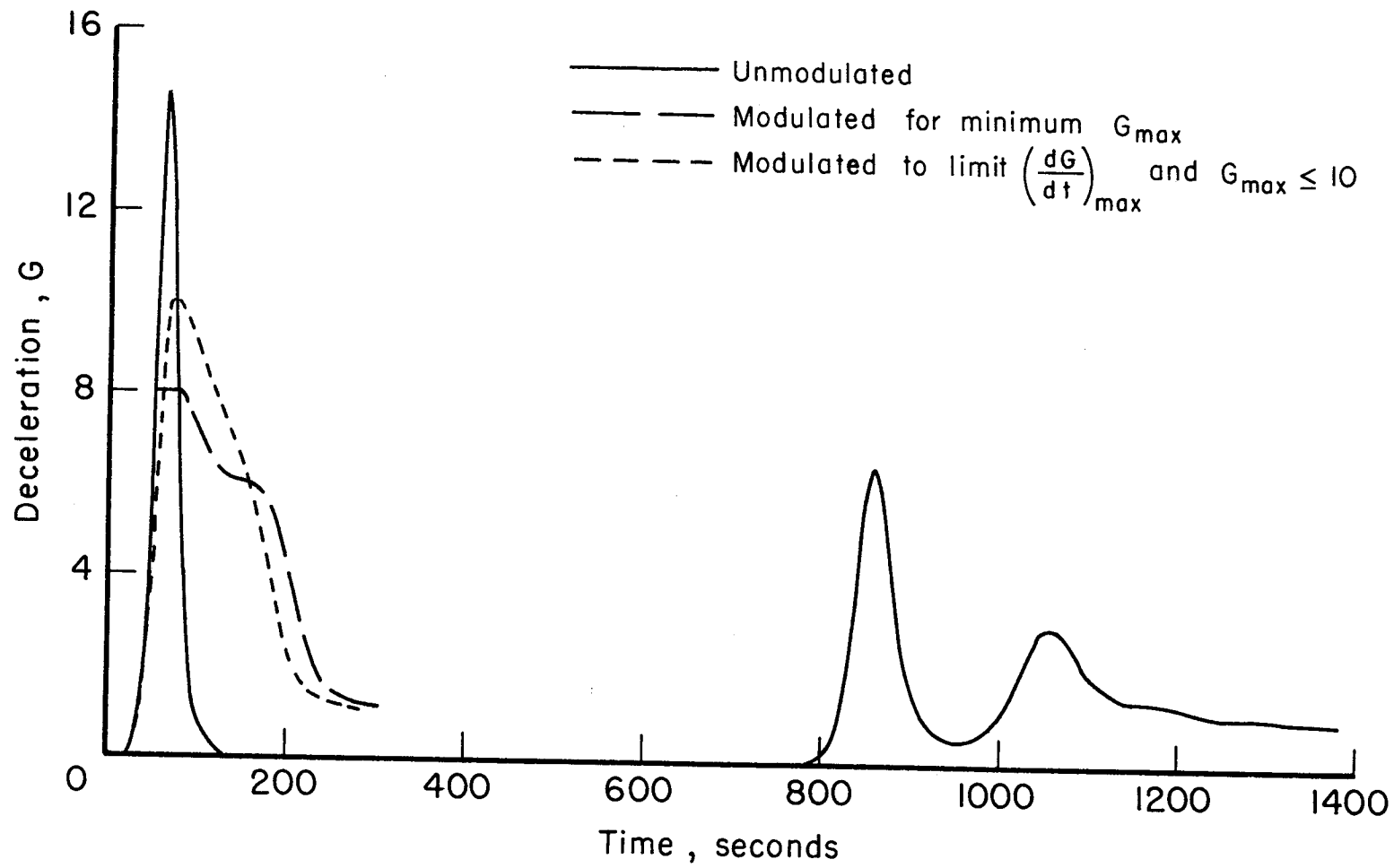
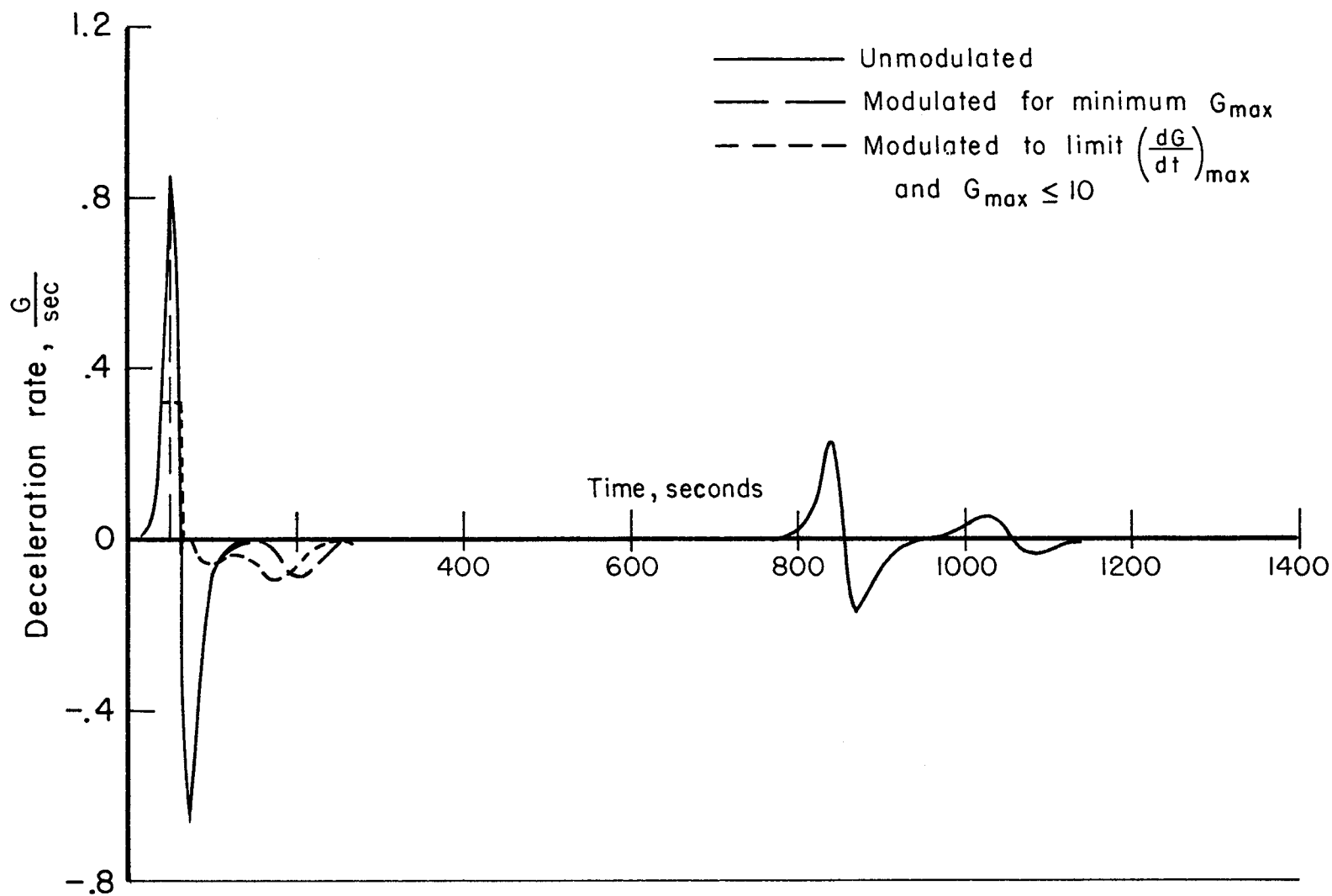


Figure 2.- Vacuum perigee altitude and corridor depth as functions of flight-path angle;  $y_i = 400,000$  ft,  $V_i = 36,335$  ft/sec.



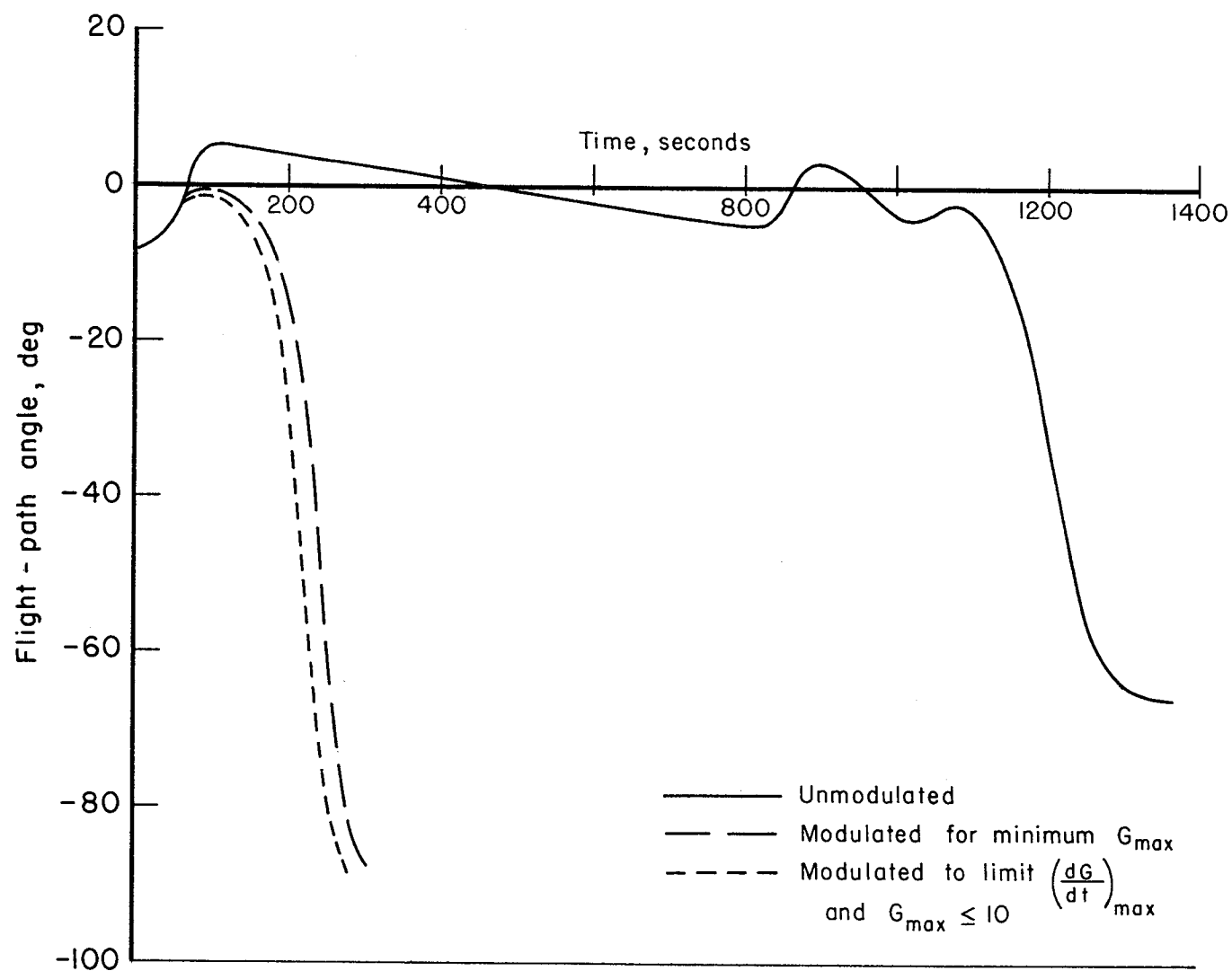
(a) Resultant deceleration

Figure 3.- Effect of modulation on entry trajectory parameters;  $V_i = 36,335$  ft/sec,  $y_i = 400,000$  ft,  $\gamma_i = -8.14^\circ$  ( $\Delta y_p = 50$  miles),  $(L/D)_i = 0.42$ ,  $m/A = 3$ .



(b) Deceleration rate

Figure 3.- Continued.



(c) Flight-path angle

Figure 3.- Continued.

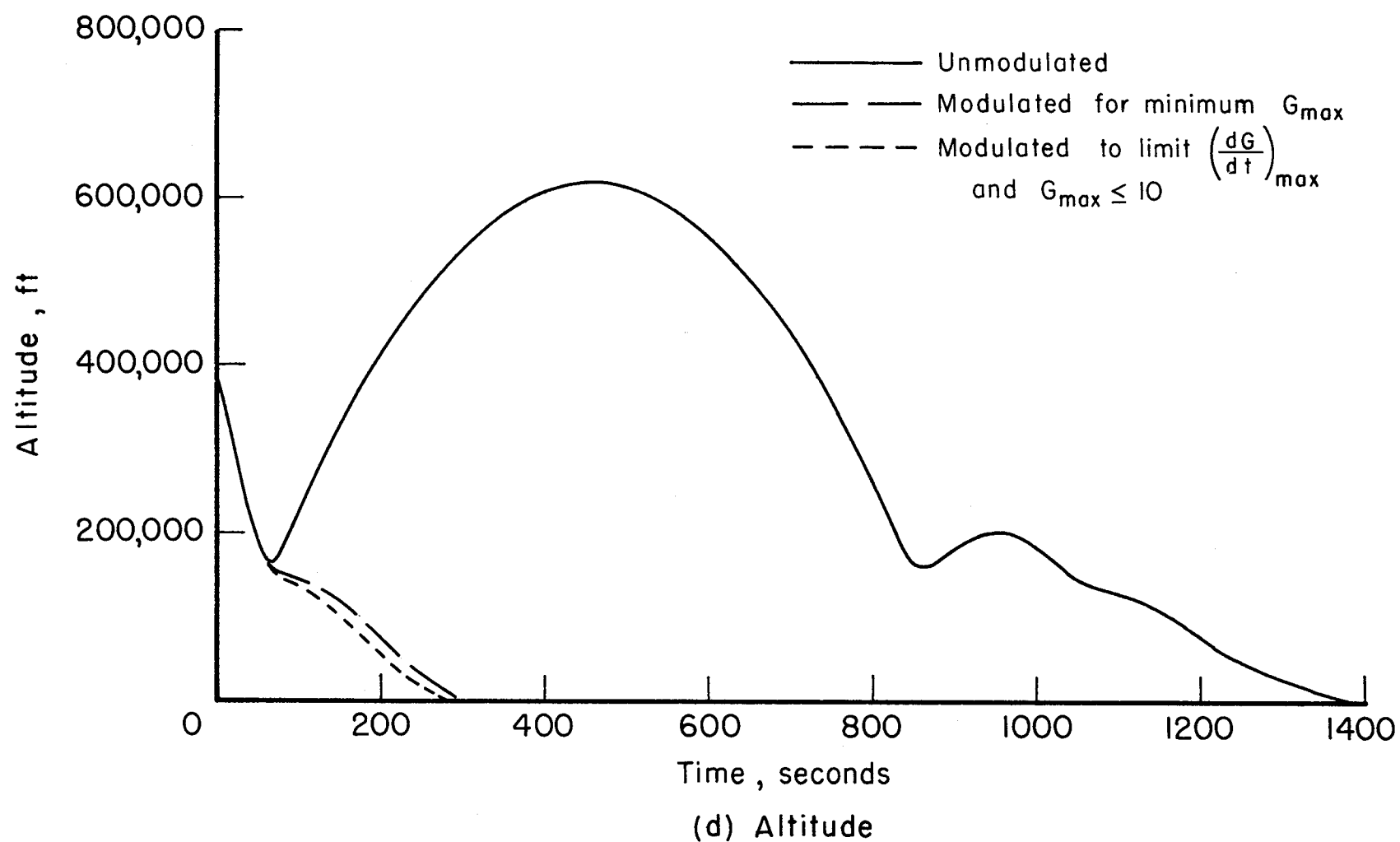
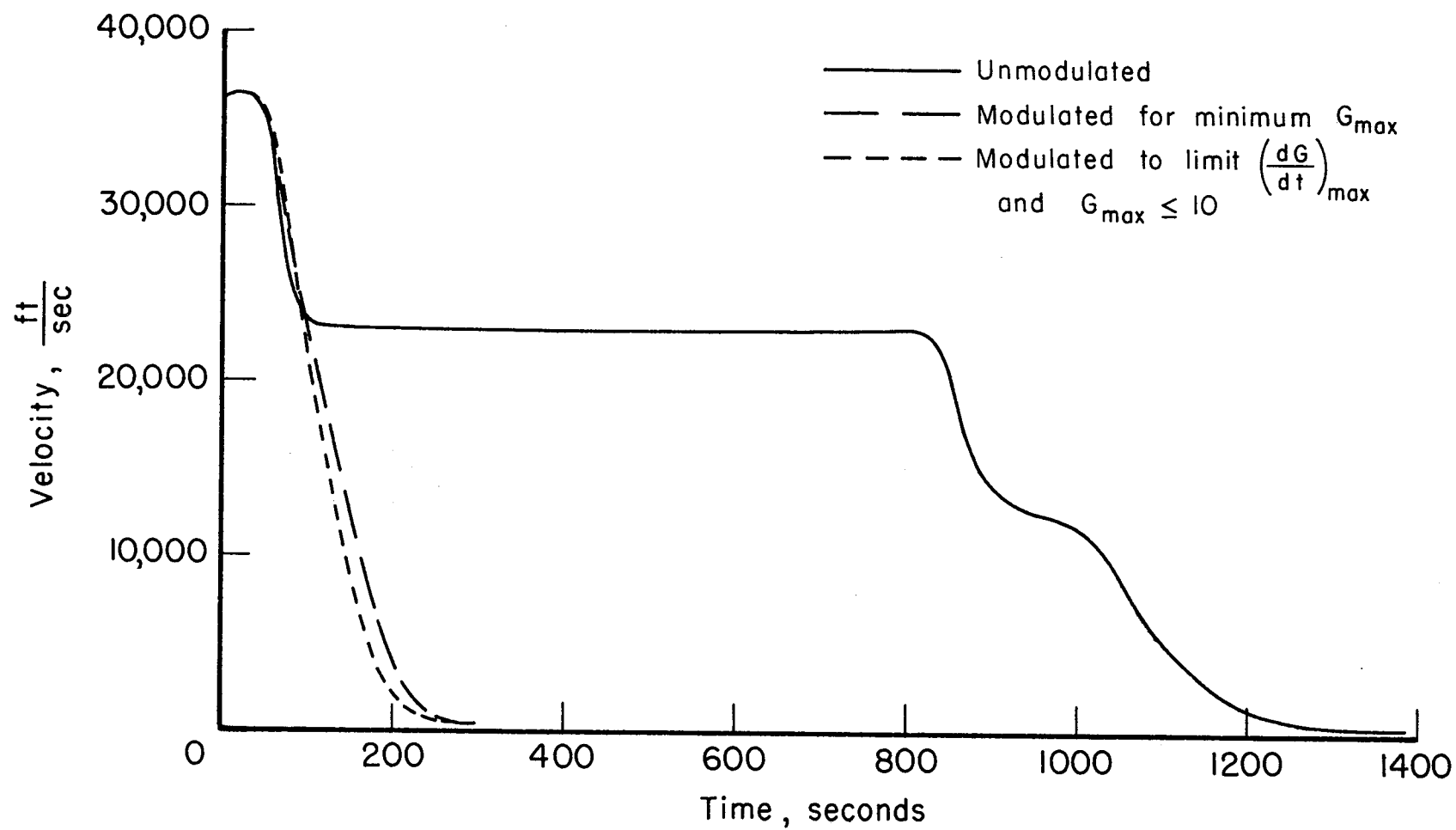


Figure 3.- Continued.



(e) Velocity

Figure 3.- Continued.

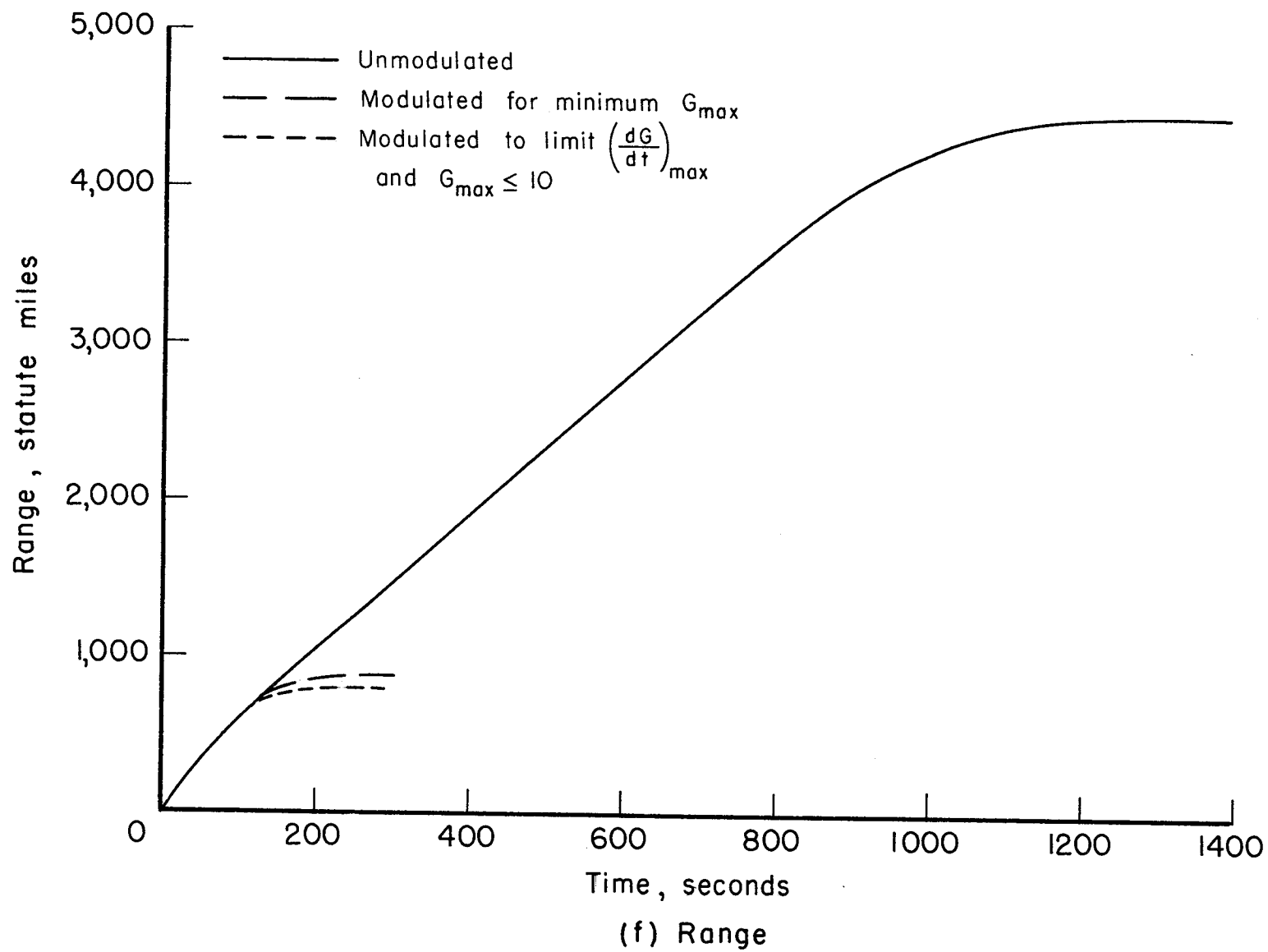
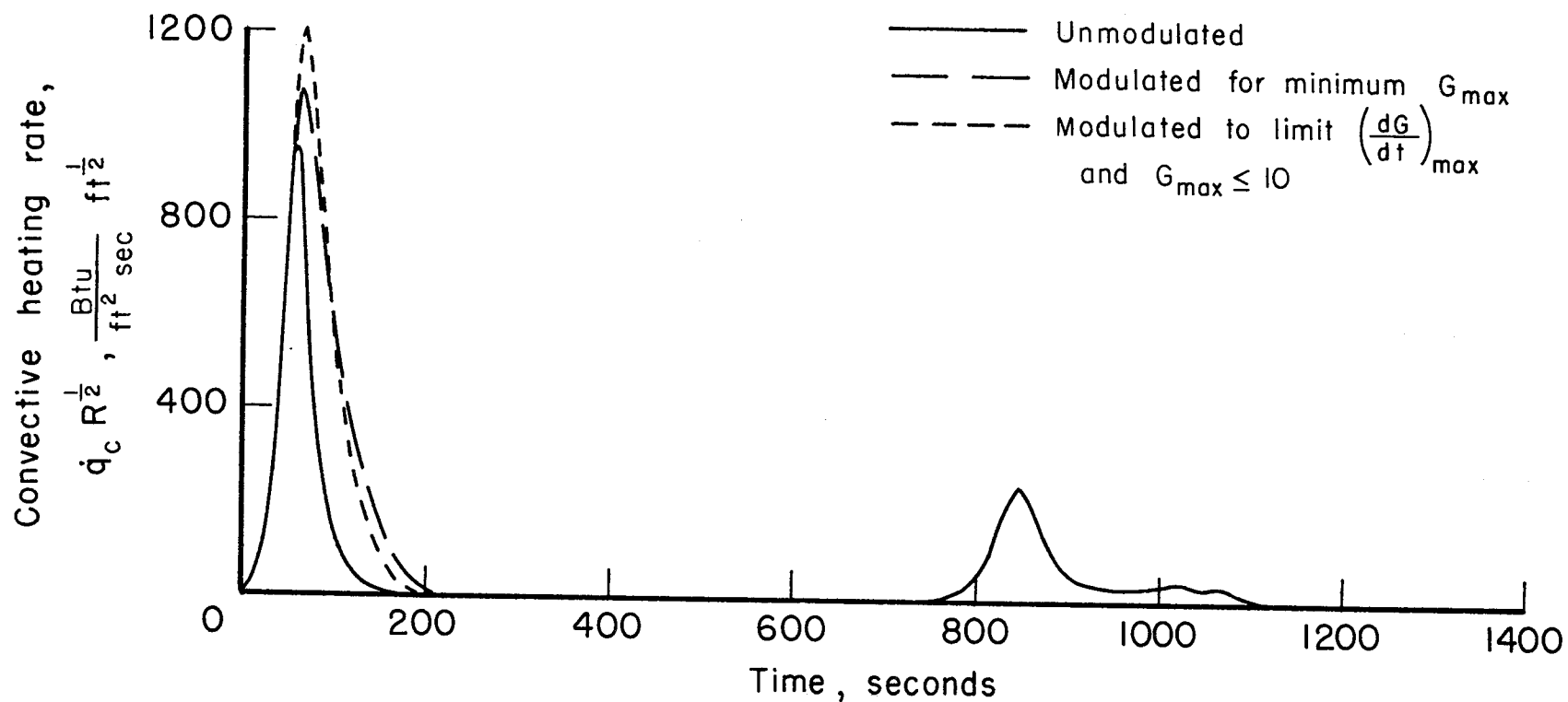


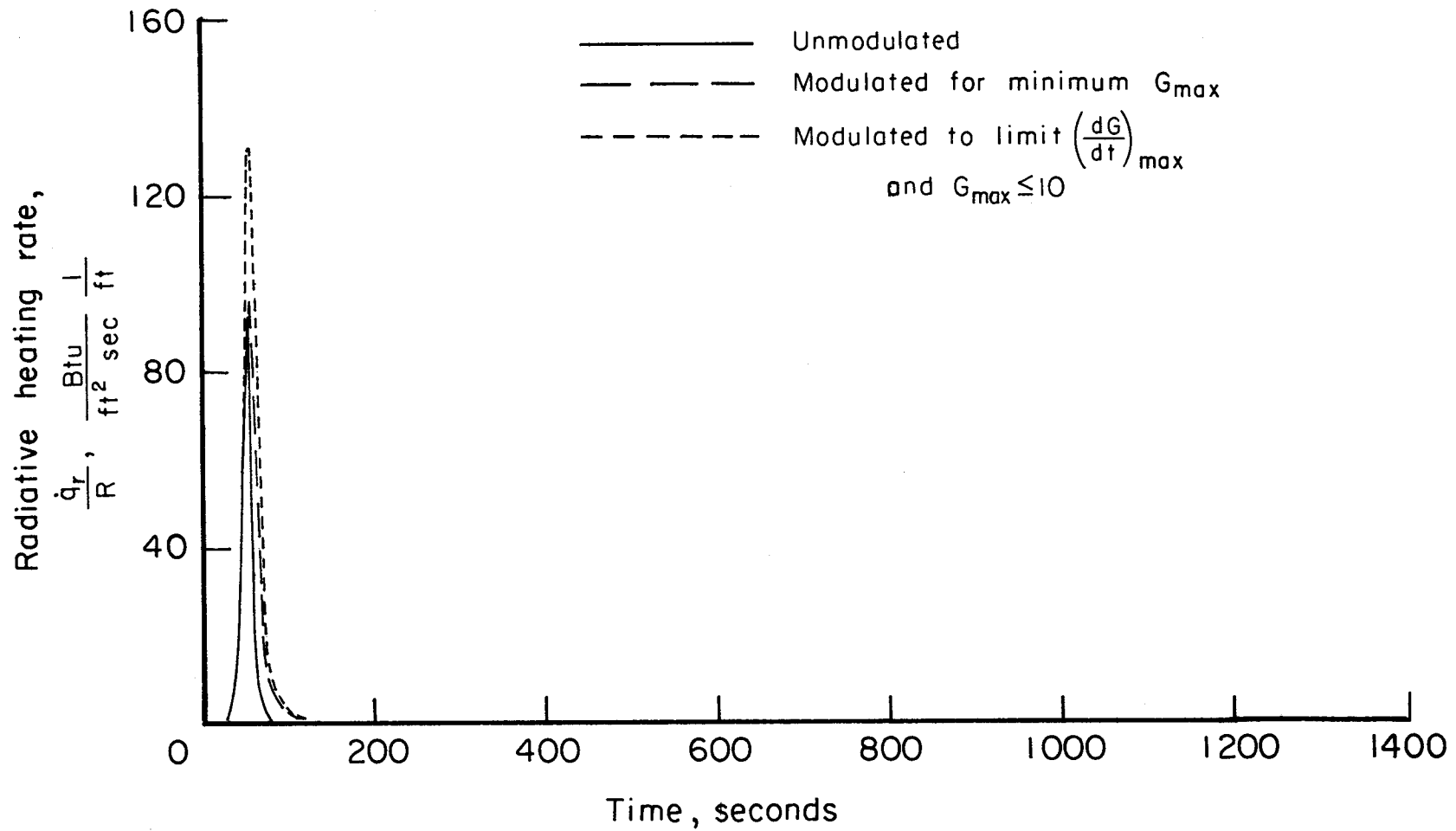
Figure 3.- Continued.



(g) Laminar convective heating rate at the stagnation point.

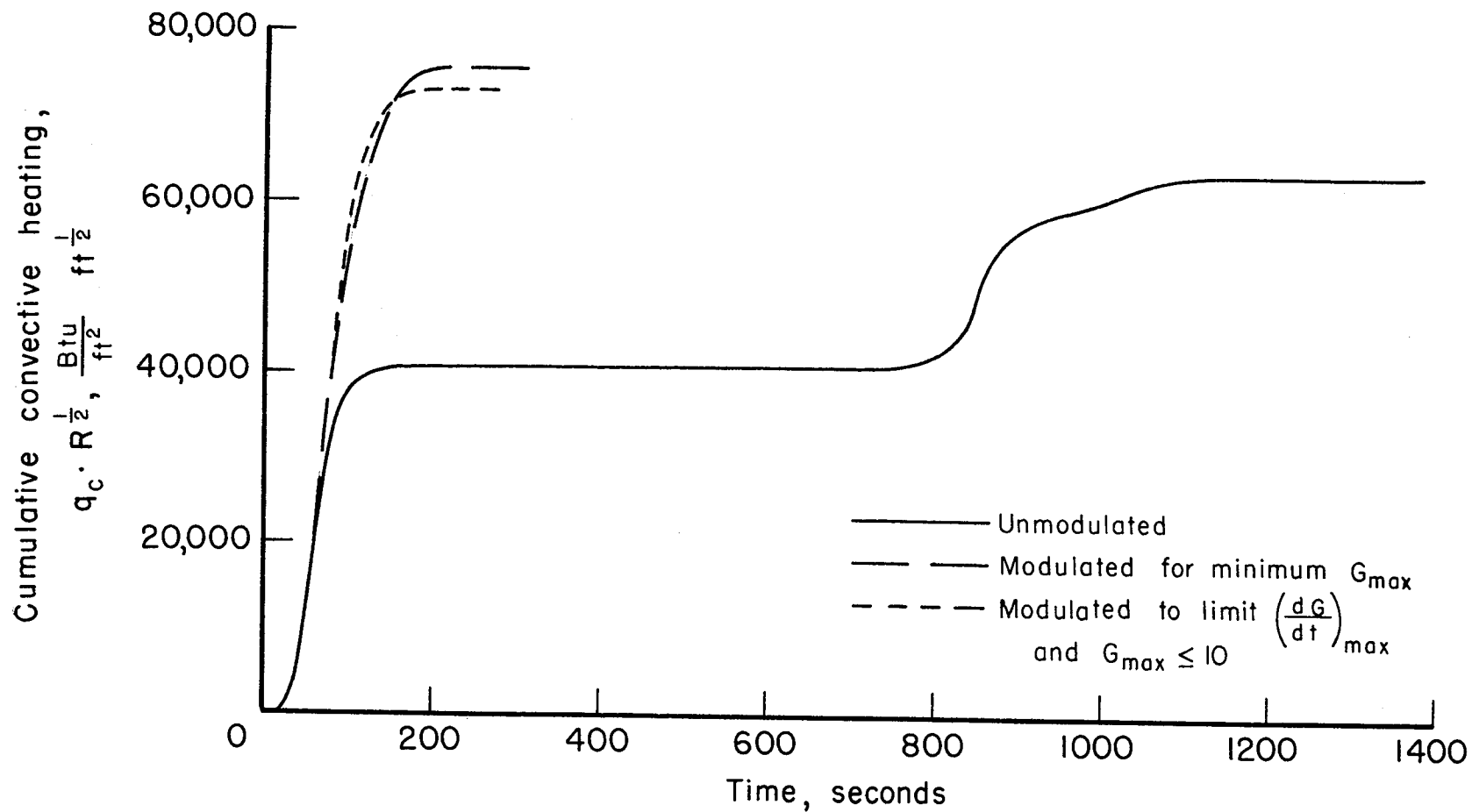
Figure 3.- Continued.





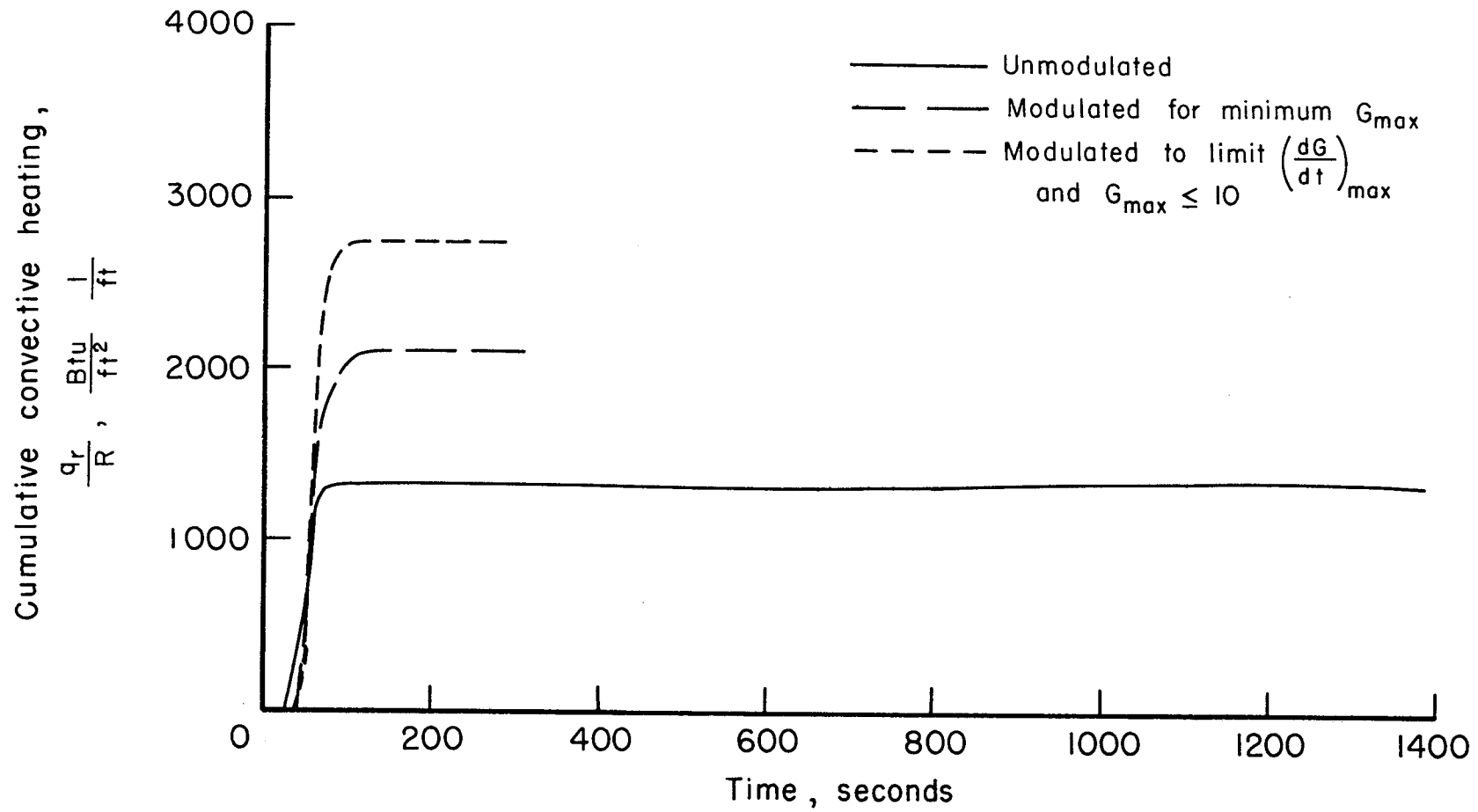
(h) Equilibrium radiative heating rate at the stagnation point.

Figure 3.- Continued.



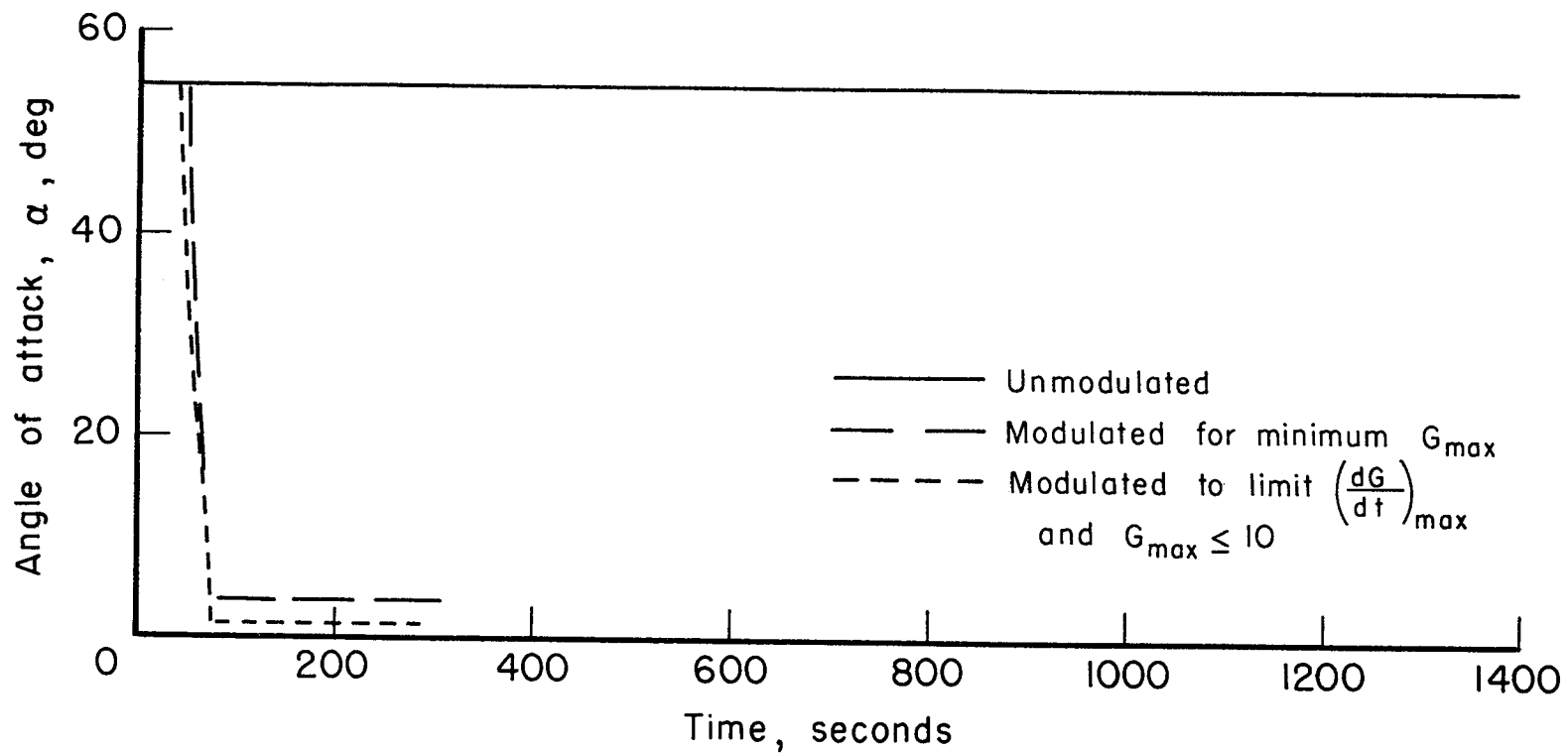
(i) Cumulative laminar convective heating at the stagnation point.

Figure 3.- Continued.



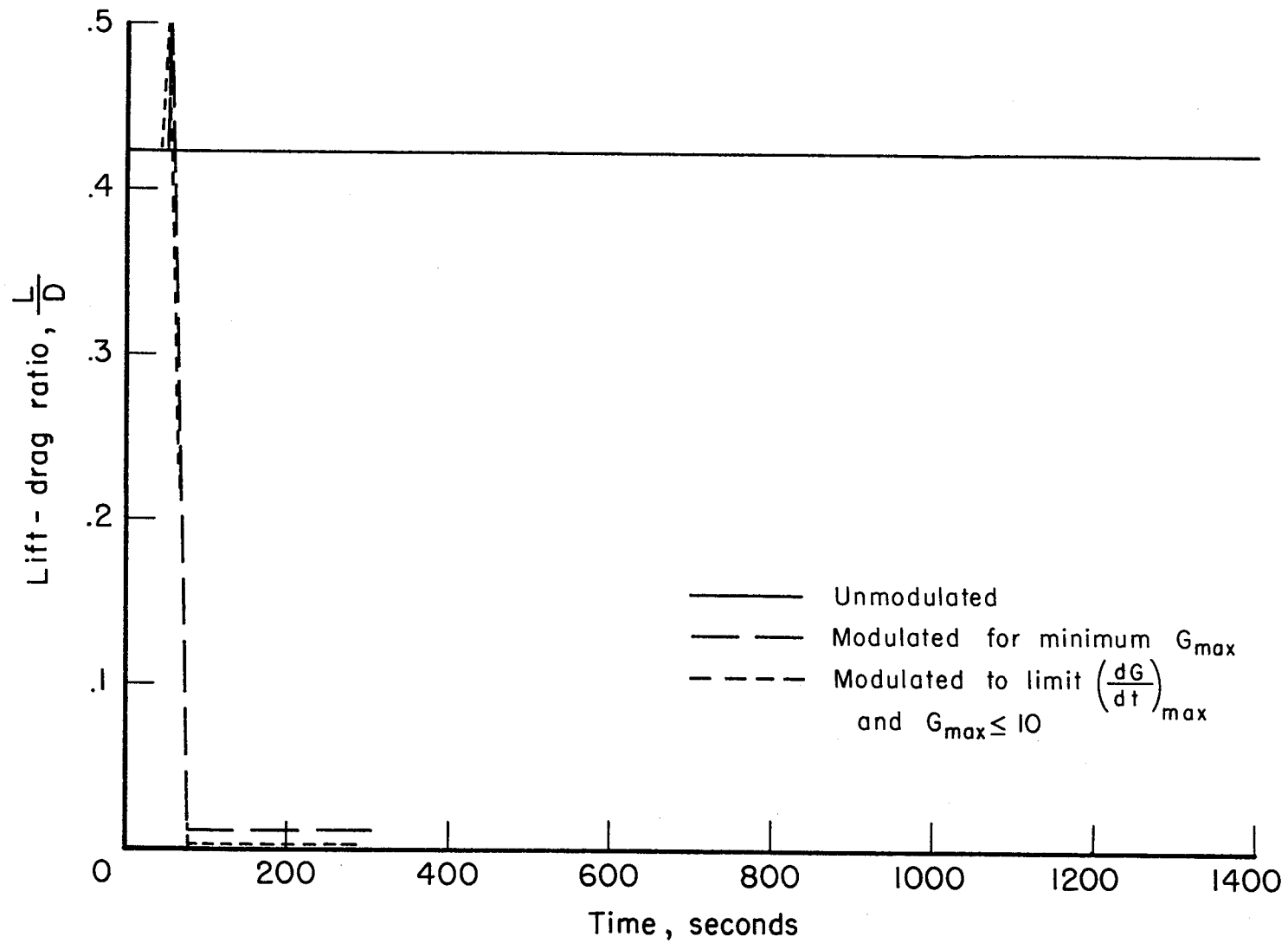
(j) Cumulative equilibrium radiative heating at the stagnation point.

Figure 3.- Continued.



(k) Angle of attack

Figure 3.- Continued.



(I) Lift - drag ratio

Figure 3.- Concluded.

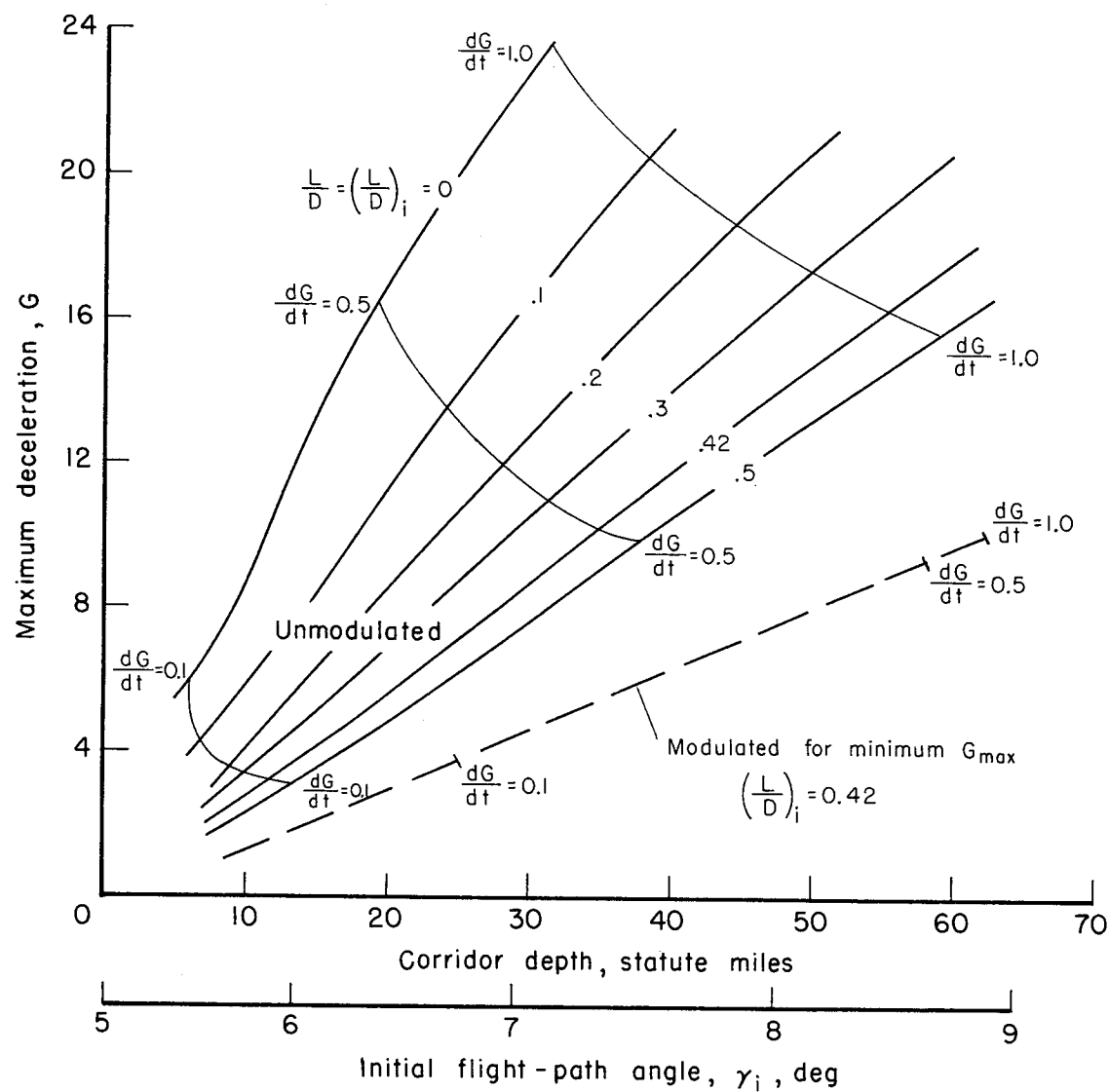


Figure 4.- Maximum decelerations for unmodulated and modulated entries;  $V_i = 36,335$  ft/sec,  $y_i = 400,000$  ft,  $m/A = 3$ .

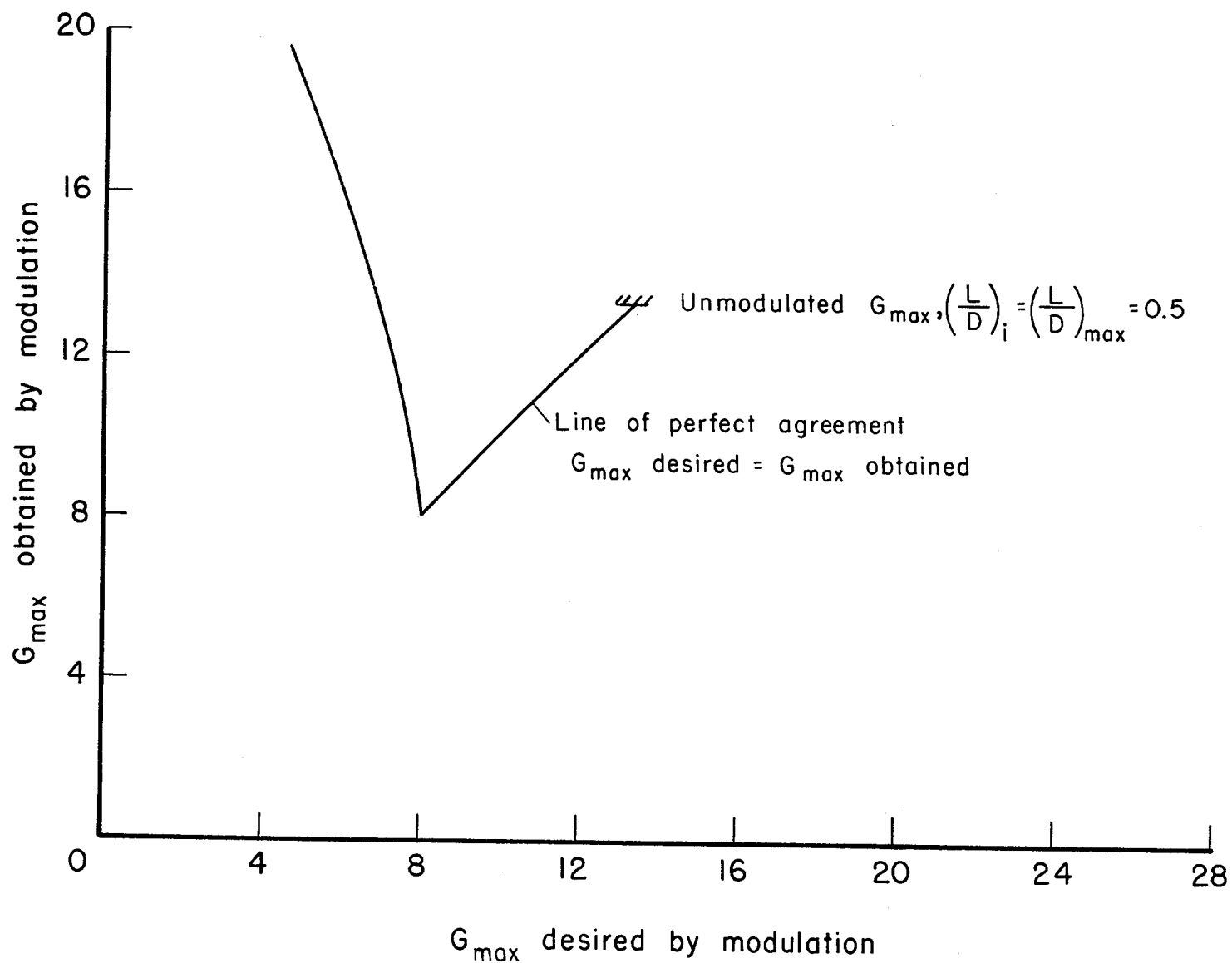


Figure 5.- Maximum deceleration obtained versus maximum deceleration desired;  $V_i = 36,335$  ft/sec,  $y_i = 400,000$  ft,  $\gamma_i = -8.14^\circ$  (50 mile corridor),  $m/A = 3$ .

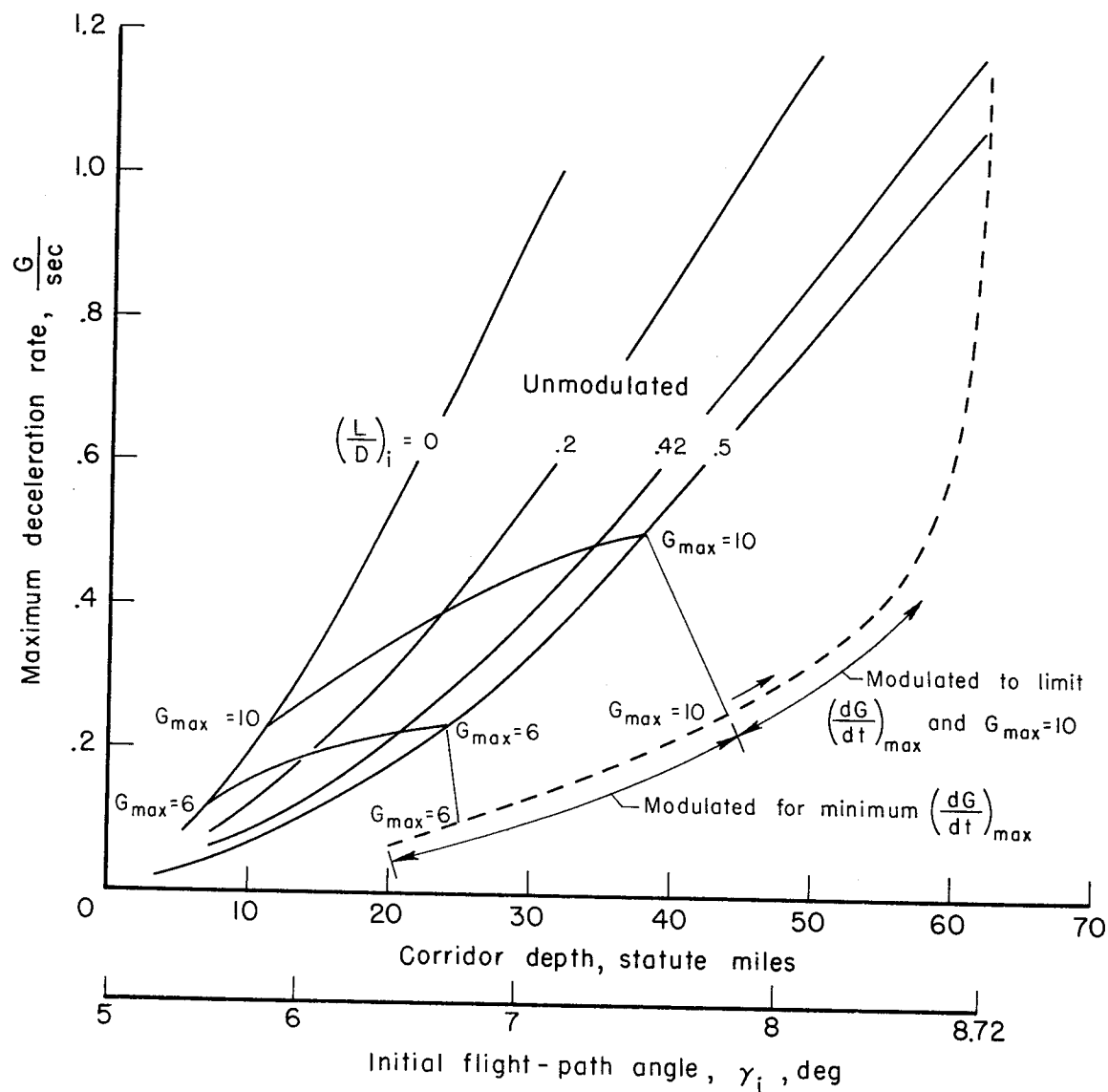


Figure 6.- Maximum deceleration rates for unmodulated and modulated entries;  $V_1 = 36,335 \text{ ft/sec}$ ,  $y_1 = 400,000 \text{ ft}$ ,  $m/A = 3$ .



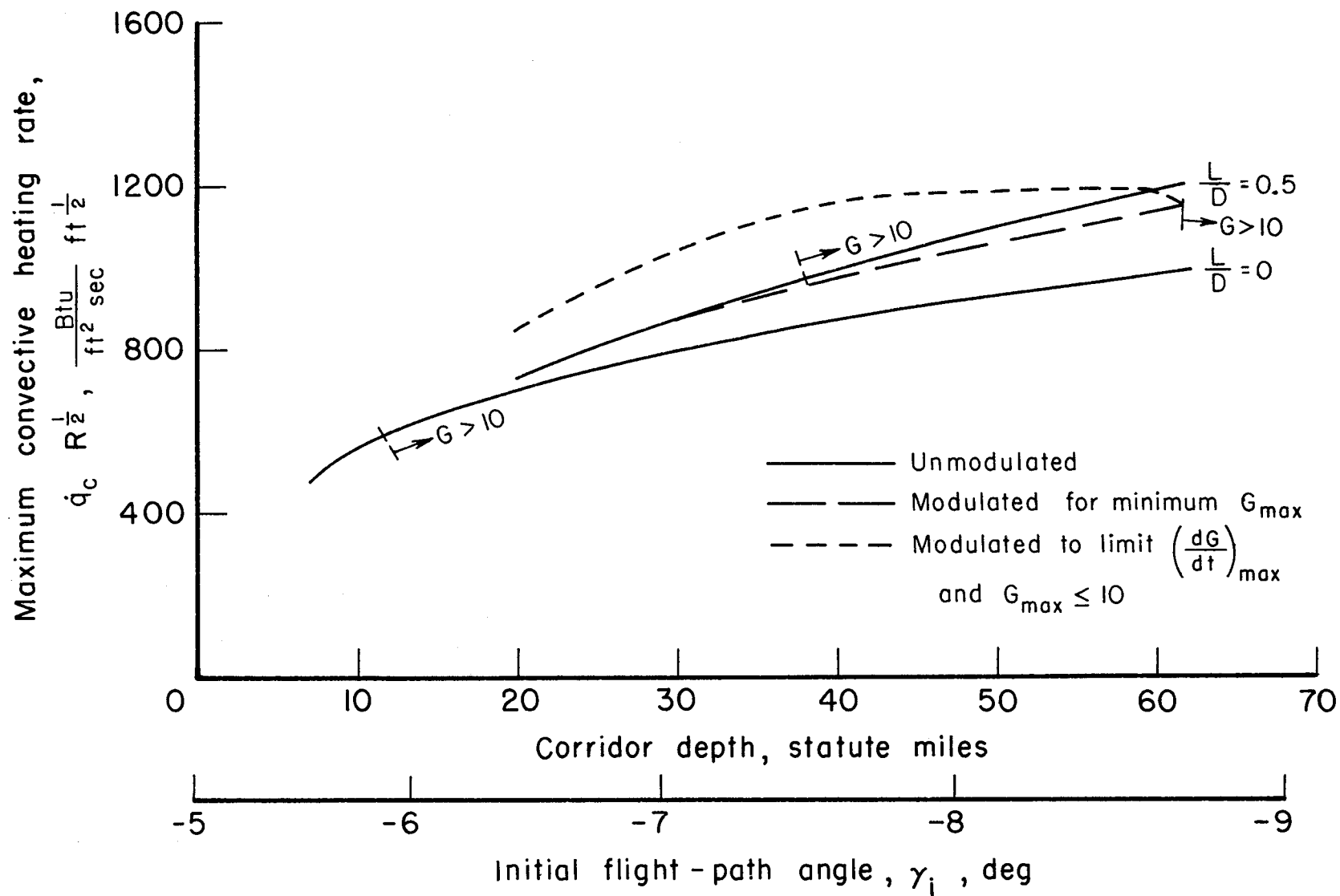


Figure 7.- Maximum laminar convective heating rates for unmodulated and modulated entries;  
 $V_1 = 36,335 \text{ ft/sec}$ ,  $y_1 = 400,000 \text{ ft}$ ,  $m/A = 3$ .

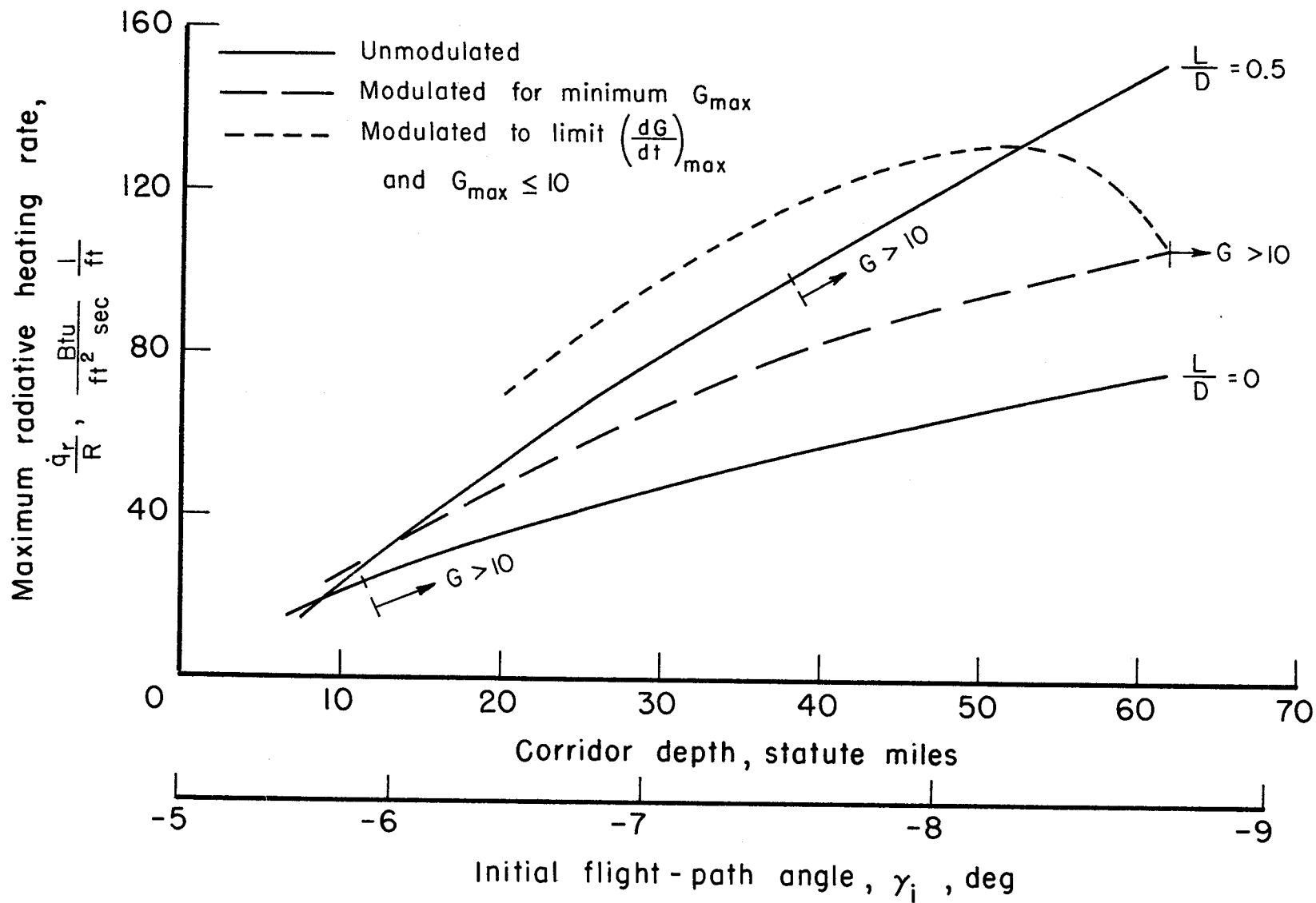


Figure 8.- Maximum equilibrium radiative heating rates for unmodulated and modulated entries;  
 $V_i = 36,335 \text{ ft/sec}$ ,  $y_i = 400,000 \text{ ft}$ ,  $m/A = 3$ .

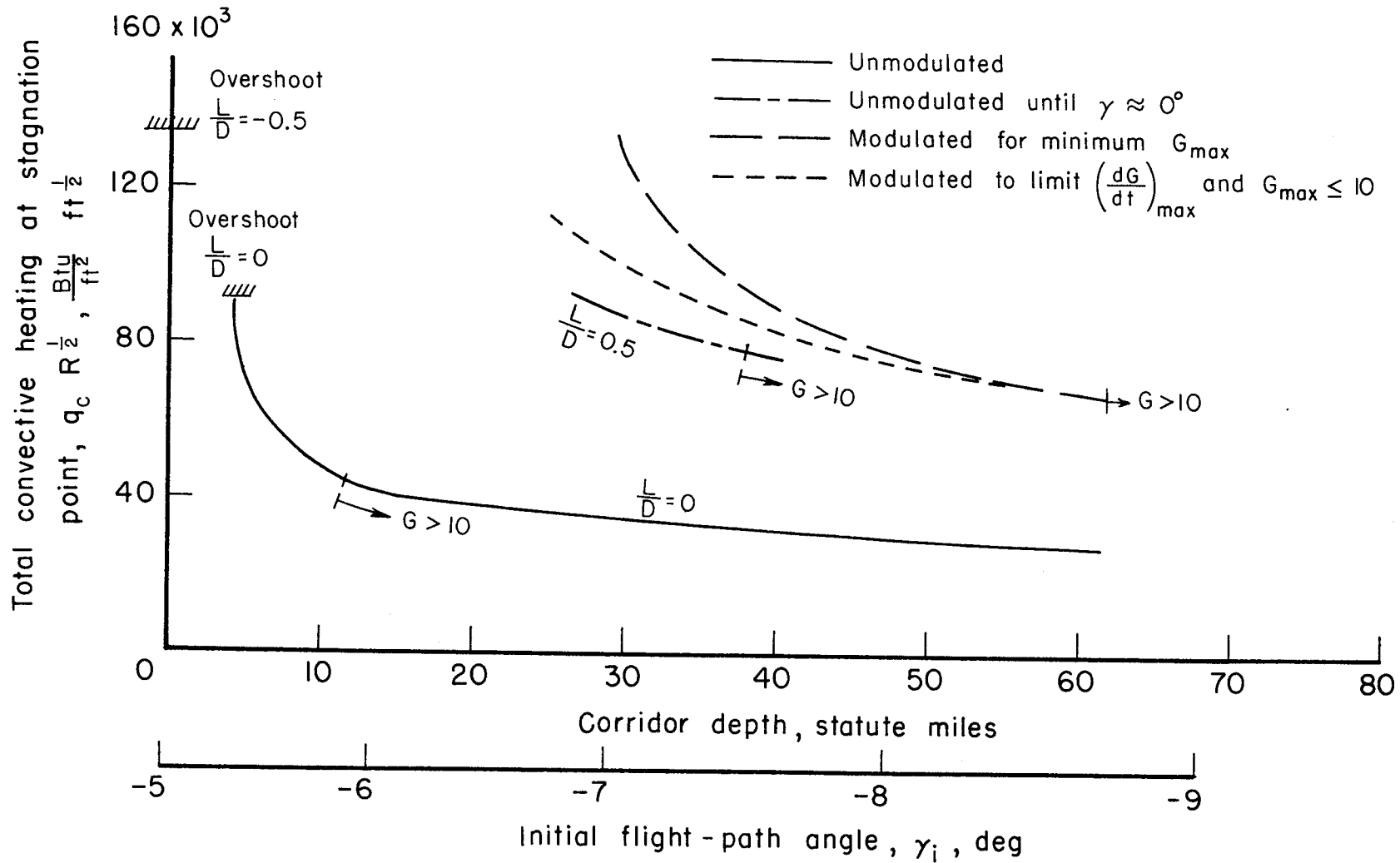


Figure 9.- Total laminar convective heating at stagnation point for unmodulated and modulated entries;  $V_i = 36,335$  ft/sec,  $y_i = 400,000$  ft,  $m/A = 3$ .

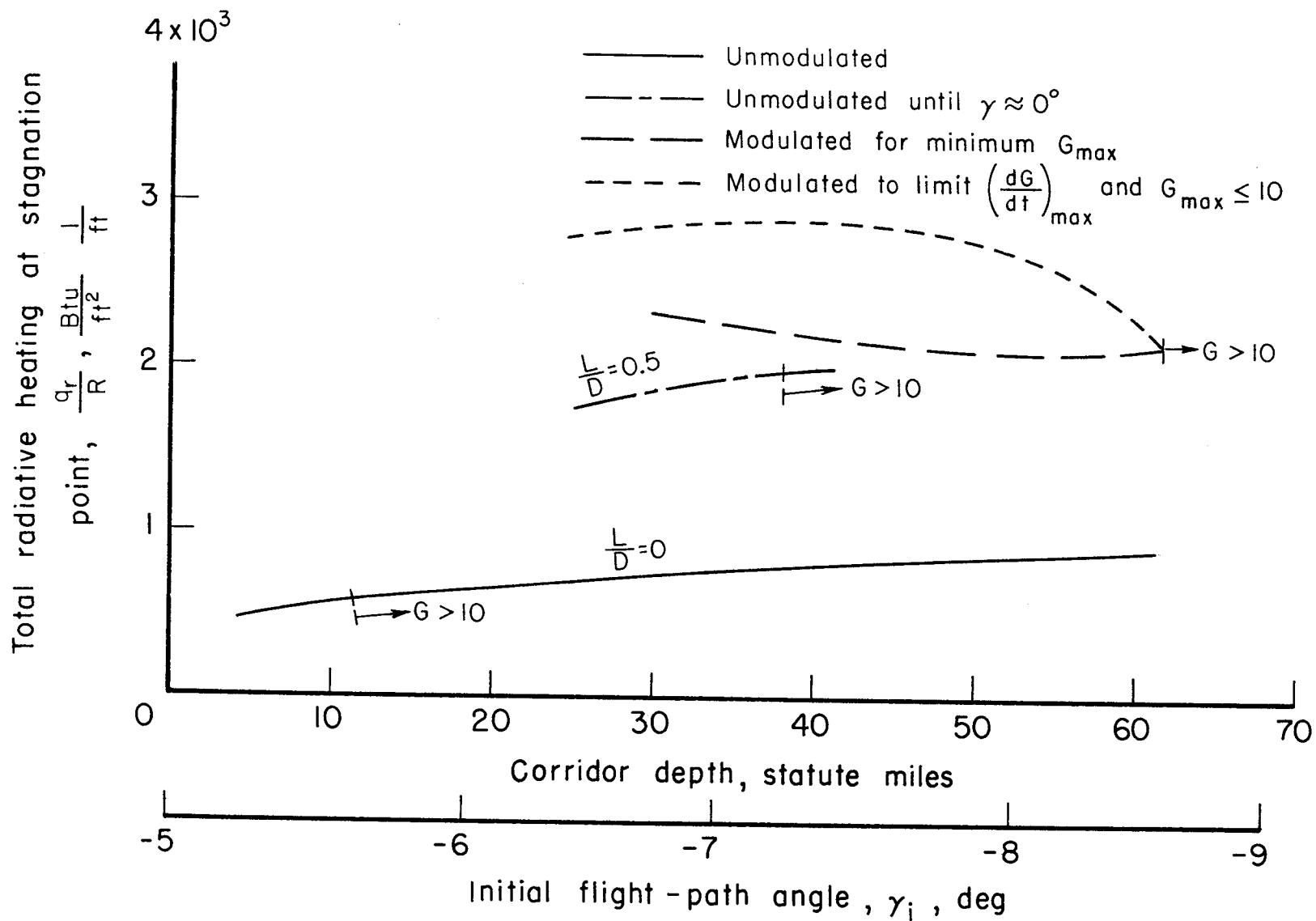


Figure 10.- Total equilibrium radiative heating at stagnation point for unmodulated and modulated entries;  $V_i = 36,335$  ft/sec,  $y_i = 400,000$  ft,  $m/A = 3$ .

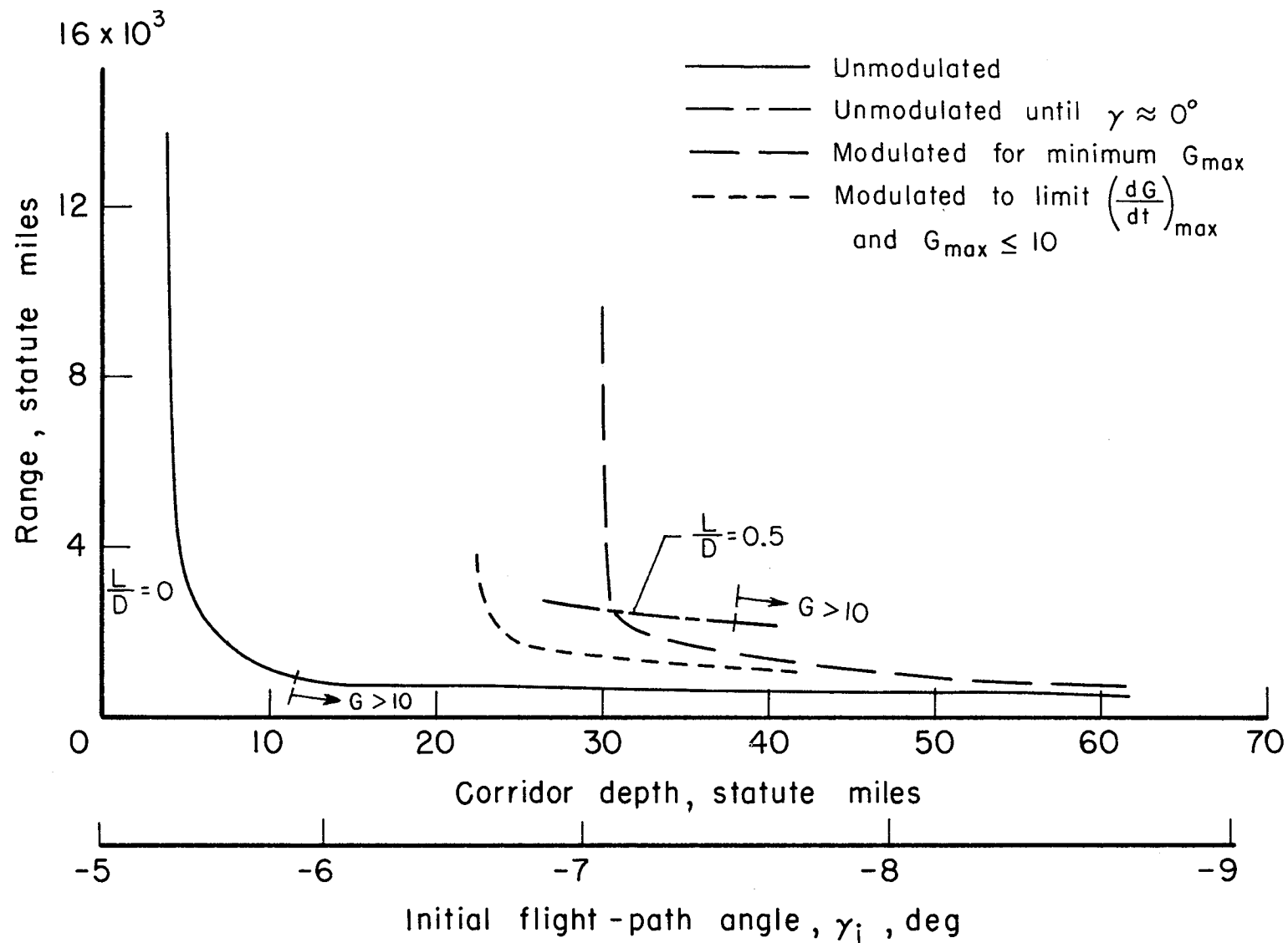


Figure 11.- Range for unmodulated and modulated entries;  $V_i = 36,335$  ft/sec,  $y_i = 400,000$  ft,  $m/A = 3$ .

NASA TN D-1145

National Aeronautics and Space Administration.  
ATMOSPHERE ENTRIES WITH VEHICLE LIFT-DRAG  
RATIO MODULATED TO LIMIT DECELERATION  
AND RATE OF DECELERATION - VEHICLES WITH  
MAXIMUM LIFT-DRAG RATIO OF 0.5. Elliott D.  
Katzen and Lionel L. Levy, Jr. December 1961.  
34p. OTS price, \$1.00.  
(NASA TECHNICAL NOTE D-1145)

Unmodulated and modulated trajectories have been  
computed for a vehicle entering the earth's atmos-  
phere at parabolic velocity. The results indicate that  
for a given initial flight-path angle, modulation in the  
angle-of-attack range from maximum lift to minimum  
drag generally resulted in a reduction of the maximum  
deceleration to 60 percent of the unmodulated value or  
a reduction of maximum deceleration rate to less than  
50 percent of the unmodulated rate.

NASA

Copies obtainable from NASA, Washington

- I. Katzen, Elliott D.
- II. Levy, Lionel L., Jr.
- III. NASA TN D-1145

(Initial NASA distribution:  
2, Aerodynamics, missiles  
and space vehicles;  
5, Atmospheric entry.)

NASA TN D-1145

National Aeronautics and Space Administration.  
ATMOSPHERE ENTRIES WITH VEHICLE LIFT-DRAG  
RATIO MODULATED TO LIMIT DECELERATION  
AND RATE OF DECELERATION - VEHICLES WITH  
MAXIMUM LIFT-DRAG RATIO OF 0.5. Elliott D.  
Katzen and Lionel L. Levy, Jr. December 1961.  
34p. OTS price, \$1.00.  
(NASA TECHNICAL NOTE D-1145)

Unmodulated and modulated trajectories have been  
computed for a vehicle entering the earth's atmos-  
phere at parabolic velocity. The results indicate that  
for a given initial flight-path angle, modulation in the  
angle-of-attack range from maximum lift to minimum  
drag generally resulted in a reduction of the maximum  
deceleration to 60 percent of the unmodulated value or  
a reduction of maximum deceleration rate to less than  
50 percent of the unmodulated rate.

NASA

Copies obtainable from NASA, Washington

- I. Katzen, Elliott D.
- II. Levy, Lionel L., Jr.
- III. NASA TN D-1145

(Initial NASA distribution:  
2, Aerodynamics, missiles  
and space vehicles;  
5, Atmospheric entry.)

NASA TN D-1145

National Aeronautics and Space Administration.  
ATMOSPHERE ENTRIES WITH VEHICLE LIFT-DRAG  
RATIO MODULATED TO LIMIT DECELERATION  
AND RATE OF DECELERATION - VEHICLES WITH  
MAXIMUM LIFT-DRAG RATIO OF 0.5. Elliott D.  
Katzen and Lionel L. Levy, Jr. December 1961.  
34p. OTS price, \$1.00.  
(NASA TECHNICAL NOTE D-1145)

Unmodulated and modulated trajectories have been  
computed for a vehicle entering the earth's atmos-  
phere at parabolic velocity. The results indicate that  
for a given initial flight-path angle, modulation in the  
angle-of-attack range from maximum lift to minimum  
drag generally resulted in a reduction of the maximum  
deceleration to 60 percent of the unmodulated value or  
a reduction of maximum deceleration rate to less than  
50 percent of the unmodulated rate.

NASA

Copies obtainable from NASA, Washington

- I. Katzen, Elliott D.
- II. Levy, Lionel L., Jr.
- III. NASA TN D-1145

(Initial NASA distribution:  
2, Aerodynamics, missiles  
and space vehicles;  
5, Atmospheric entry.)

NASA TN D-1145

National Aeronautics and Space Administration.  
ATMOSPHERE ENTRIES WITH VEHICLE LIFT-DRAG  
RATIO MODULATED TO LIMIT DECELERATION  
AND RATE OF DECELERATION - VEHICLES WITH  
MAXIMUM LIFT-DRAG RATIO OF 0.5. Elliott D.  
Katzen and Lionel L. Levy, Jr. December 1961.  
34p. OTS price, \$1.00.  
(NASA TECHNICAL NOTE D-1145)

Unmodulated and modulated trajectories have been  
computed for a vehicle entering the earth's atmos-  
phere at parabolic velocity. The results indicate that  
for a given initial flight-path angle, modulation in the  
angle-of-attack range from maximum lift to minimum  
drag generally resulted in a reduction of the maximum  
deceleration to 60 percent of the unmodulated value or  
a reduction of maximum deceleration rate to less than  
50 percent of the unmodulated rate.

NASA

Copies obtainable from NASA, Washington

- I. Katzen, Elliott D.
- II. Levy, Lionel L., Jr.
- III. NASA TN D-1145

(Initial NASA distribution:  
2, Aerodynamics, missiles  
and space vehicles;  
5, Atmospheric entry.)